# Breaking, merging and splashing bubbles: the art of fluid interface CFD

Stéphane Zaleski

*Modélisation en Mécanique, Paris VI*

http://www.lmm.jussieu.fr/~zaleski/zaleski.html

# The fascination of multiphase flow

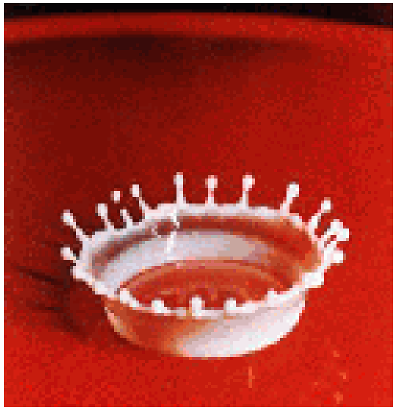
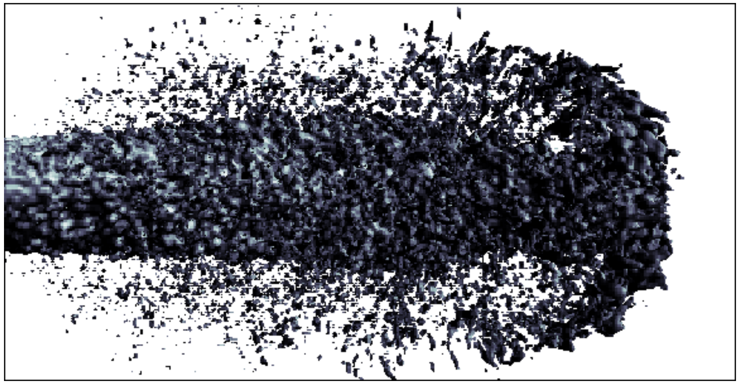
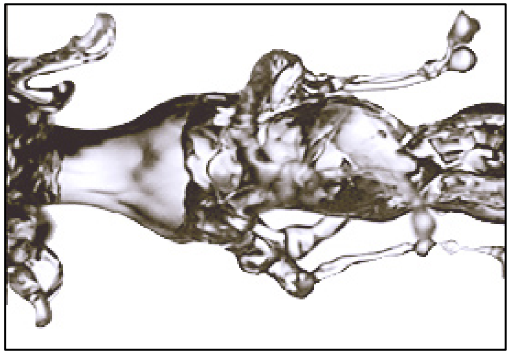
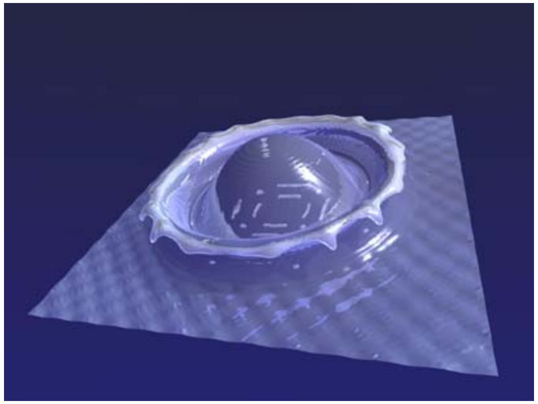

## GOVERNING EQUATIONS: NAVIER-STOKES

$$\partial_t (\rho \mathbf{u}) + \nabla \cdot (\rho \mathbf{u} \otimes \mathbf{u}) = -\nabla p + \nabla \cdot (2\mu \mathbf{D}) + \sigma \kappa \delta_S \mathbf{n} + \left( \nabla \sigma \right) \delta_S + \rho \mathbf{g},$$

where the strain-rate tensor **D** is

$$D_{ij} = \frac{1}{2} \left( \frac{\partial u_j}{\partial x_i} + \frac{\partial u_i}{\partial x_j} \right).$$

Notice new term with surface tension $\sigma$ .
Both fluids are considered incompressible

$$\nabla \cdot \mathbf{u} = 0 .$$

GOVERNING EQUATIONS: NAVIER-STOKES

Incompressibility is chosen because

- Most applications involve low Ma number flow
- Even at Ma = 0.3 compressibility effects are not the most important issue (e.g. in atomization problems)
- Simulation of compressible flows is technically much more difficult.

## GOVERNING EQUATIONS: JUMP CONDITIONS

Another way to formulate the equations is to introduce jump conditions

$\left[ X \right]$ Is the jump of X beween fluids 1 and 2.

$$\left[ X \right] = X_1 - X_2$$

Jump conditions:

a) velocity $\left[ \mathbf{u} \right] = 0$

b) Momentum flux: $\left[ \left( p\mathbf{1} + 2\mu\mathbf{D} \right) \cdot \mathbf{n} \right] = \sigma\mathbf{n} + \nabla\sigma$

## GOVERNING EQUATIONS: KINEMATICS

The interface S follows the flow. Its normal velocity is

$$V_S = \mathbf{u} \cdot \mathbf{n} \, .$$

Another useful formulation involves the characteristic function $\chi$.

$$\partial_t \chi + \mathbf{u} \cdot \nabla \chi = 0$$

This equation inspires both VOF and level-set methods

If $\chi$ =1 in phase 1 and $\chi$ =0 in phase 2: VOF , if $\chi$ = distance, Level Set. VOF and level set share a lot of characteristics.

# DEFINITION OF THE VOF METHOD

True interface

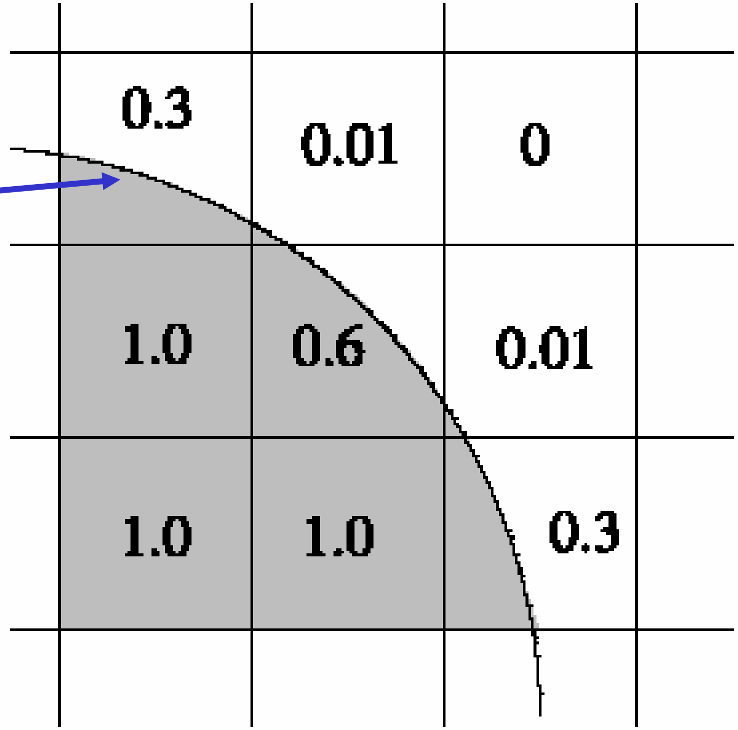


$C_{ij}$ = Volume of « fluid » in cell ij

# THE SIMPLEST VOF METHOD

Let $\chi$ =1 in phase 1 and $\chi$ =0 in phase 2. Then solve

$$\partial_t \chi + \mathbf{u} \cdot \nabla \chi = 0$$

using standard hyperbolic equations methods (e.g. TVD, FCT, ENO, Artificially compressible).

References: JADIM code (Toulouse), Issa and Ubbink.

Advantage: easy to program. Problems: interface thickens in time, lack of accuracy

# POSSIBLE GRIDS

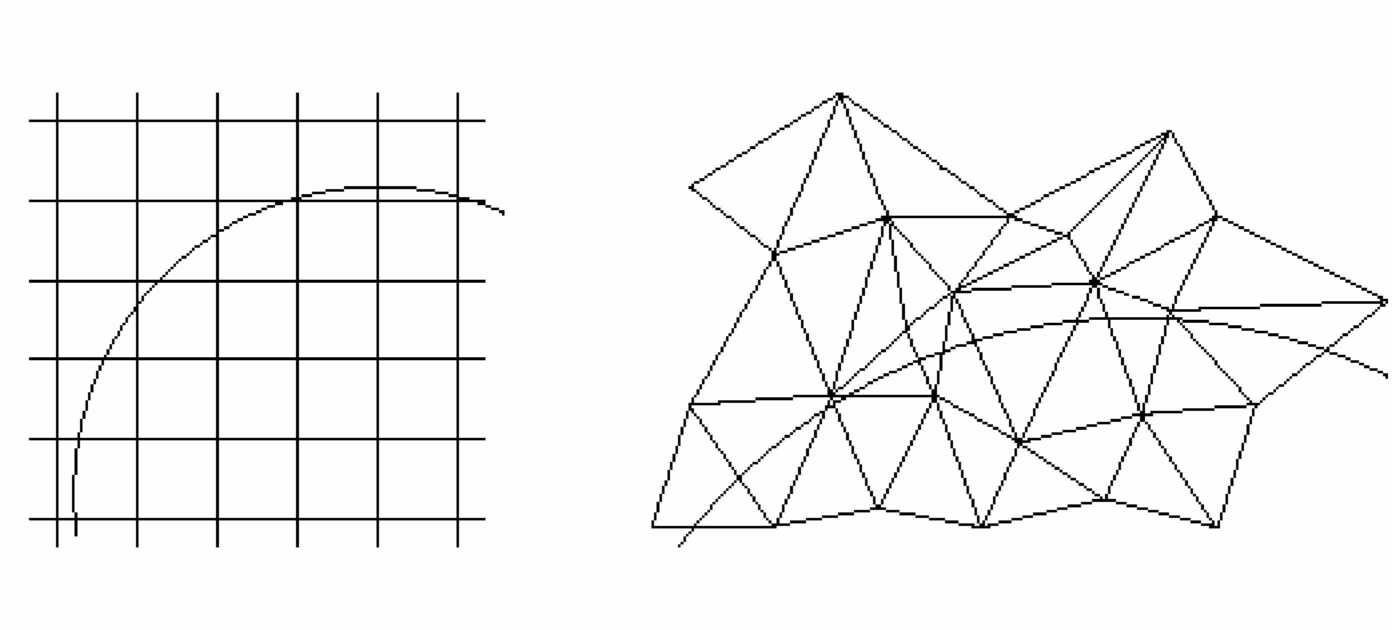

regular general, unstructured

VOF methods are not limited to regular grids, although treatment is much simpler and more accurate on regular grids.

## RECONSTRUCTION

Standard VOF methods proceed in two steps: reconstruction and propagation.

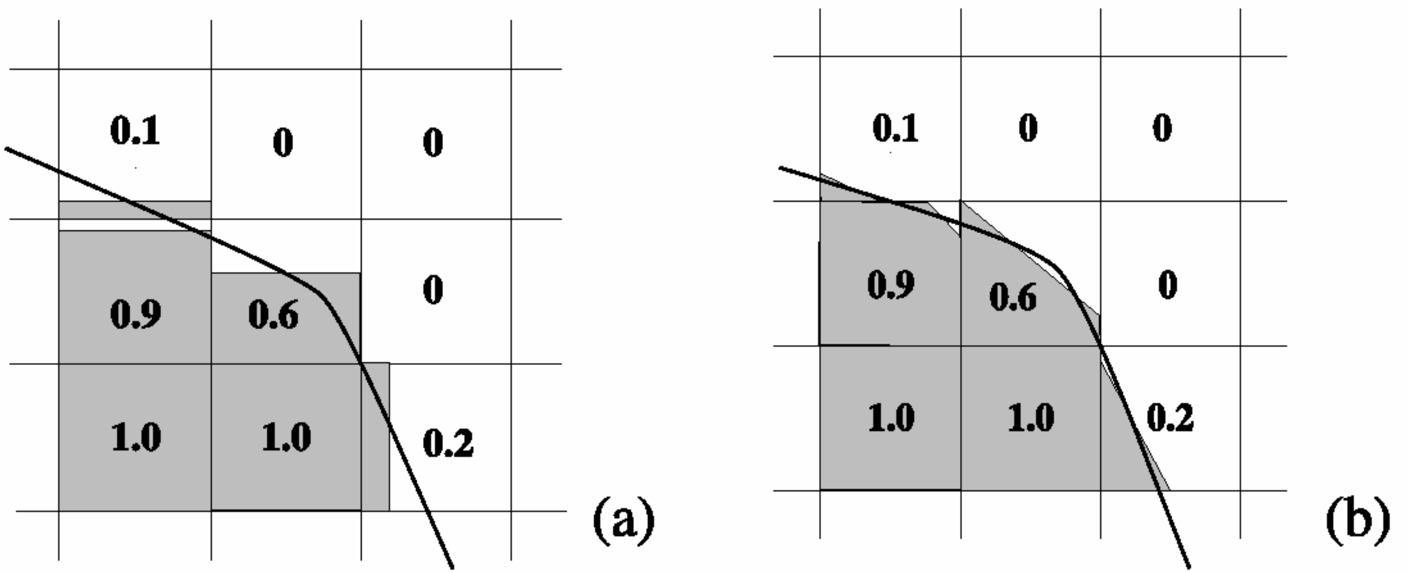


(a) is a « first order », Simple Line Interface Construction, (SLIC).
Its accuracy is similar to that obtained on unstructured grids.
(b) is a « second order » Piecewise Linear Interface Construction (PLIC)

# RECONSTRUCTION

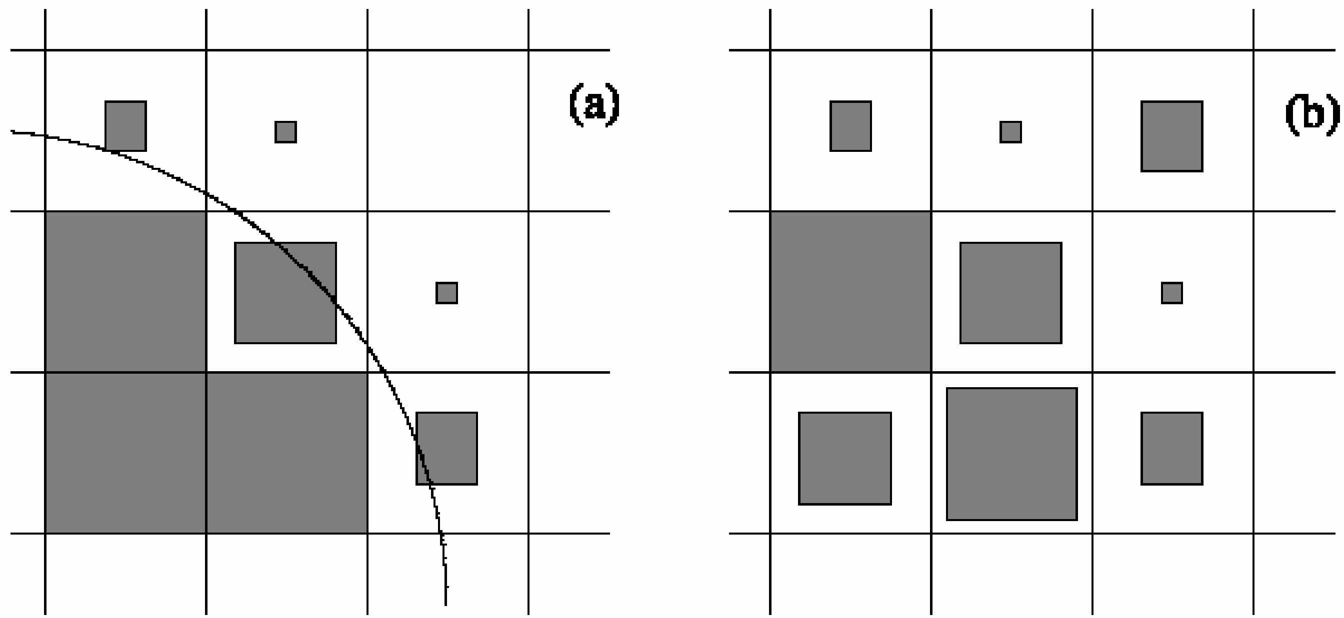


The « VOF bag problem » (after Markus Meier).
All that is known is how much mass there is in each cell.
In case (a) the interface is easier to reconstruct than in case (b)

# RECONSTRUCTION

Steps in reconstruction:

1. Determination of **n.**

- Parker and Young (P.-.Y.) or « finite difference » method.
- Puckett and Pilliod or ELVIRA least-squares method.
- Scardovelli 's linear fit method.

2. Position the interface once **n** is found and $C_{ij}$ given.

# DETERMINATION OF N: P.-Y. METHOD

Finite difference method: corner values

$$n_{x,i+1/2,j+1/2} = \frac{1}{4}\left(C_{i+1,j} + C_{i+1,j+1} - C_{i,j} - C_{i,j+1}\right)$$

$$n_{y,i+1/2,j+1/2} = \frac{1}{4}\left(C_{i,j+1} + C_{i+1,j+1} - C_{i,j} - C_{i+1,j}\right)$$

Finite difference method: cell center values

$$\mathbf{n}_{ij} = \frac{1}{4}\left(\mathbf{n}_{i+1/2\,j+1/2} + \mathbf{n}_{i-1/2,j+1/2} + \mathbf{n}_{i+1/2,j-1/2} + \mathbf{n}_{i-1/2,j-1/2}\right)$$

## DETERMINATION OF N: P.-Y. METHOD

Finite differences fail to obtain **n** exactly for a straight line in some cases such as the straight line below.

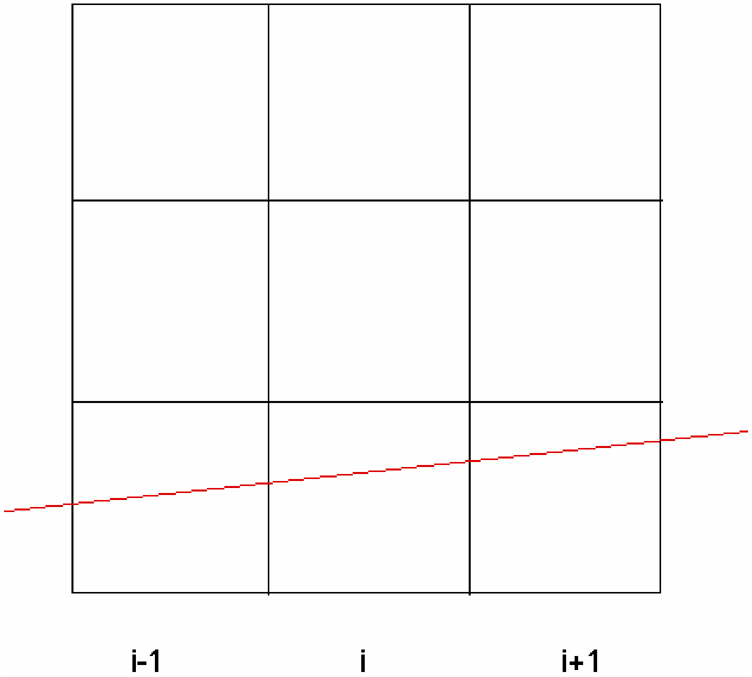

# DETERMINATION OF N: ELVIRA

ELVIRA is interesting because it is the first truly second-order method: it approximates straight lines exactly.

It works by a *least-squares fit* to the interface normal

# RECONSTRUCTION

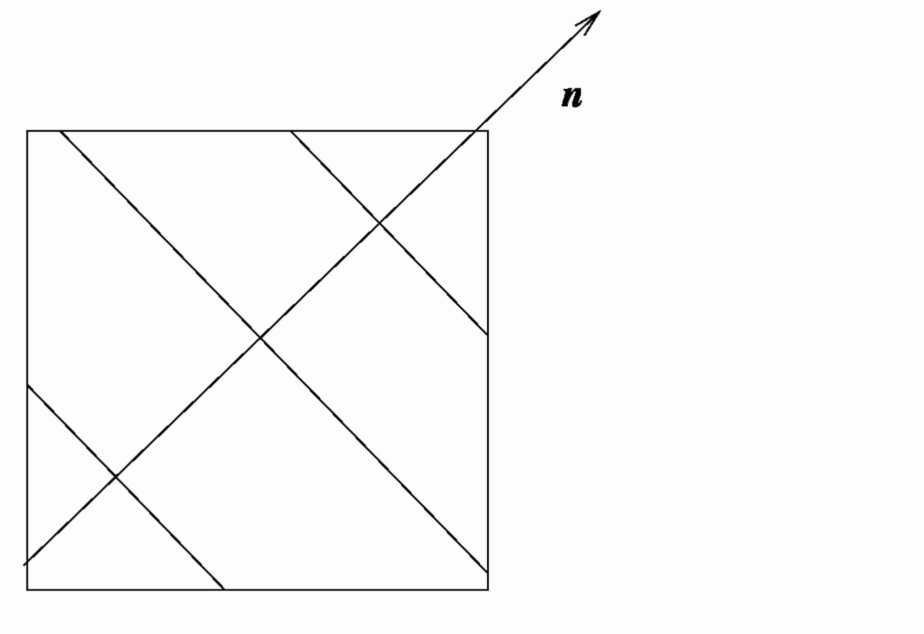


Three cases exist for an interface in a 2D cell. Once interface orientation **n** is found , the interface position may be found. The equation of the interface is **m. x** = $\alpha$ .

# RECONSTRUCTION

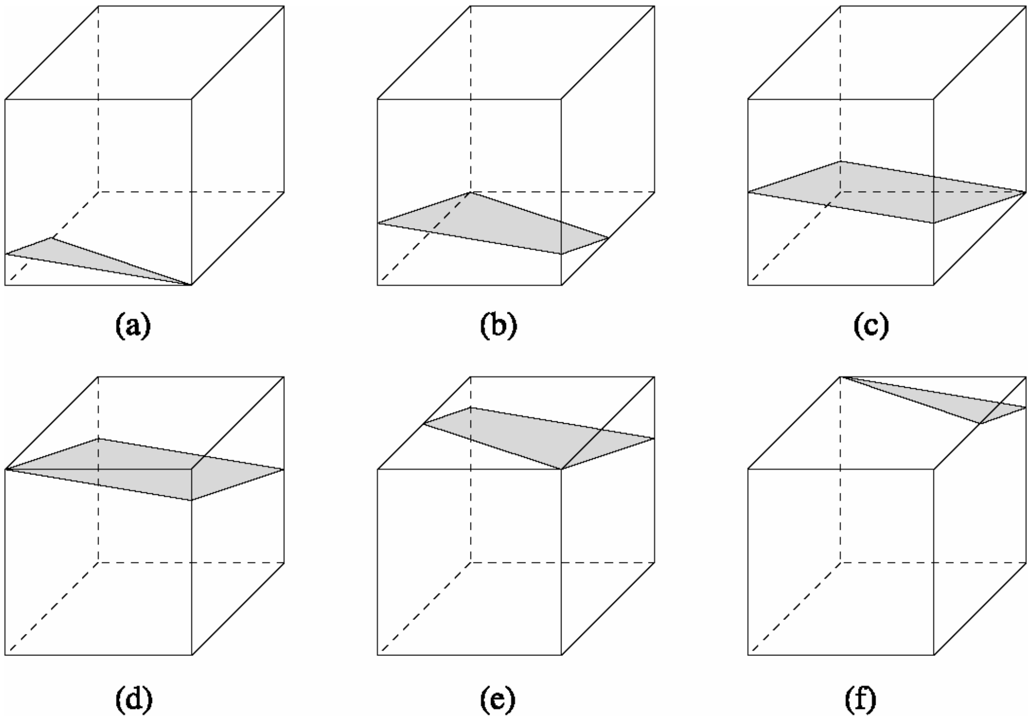


(patented ?)

# PROPAGATION

First manipulate the continuous form of the equations

$$\frac{C^{n+1}-C^{n}}{\tau}=-\partial_x(u_x C)-\partial_y(u_y C)+(\partial_x u_x)C+(\partial_y u_y)C$$

Discretize ->Naive split discrete form:

$$\frac{C_{ij}{}^{n+1/2}-C_{ij}{}^{n}}{\tau}=-D_x(u_x C^{n})=-D_x\phi_x^{n}$$

$$\frac{C_{ij}{}^{n+1}-C_{ij}{}^{n+1/2}}{\tau}=-D_y(u_y C^{n})=-D_y\phi_y^{n}$$

# Naive method

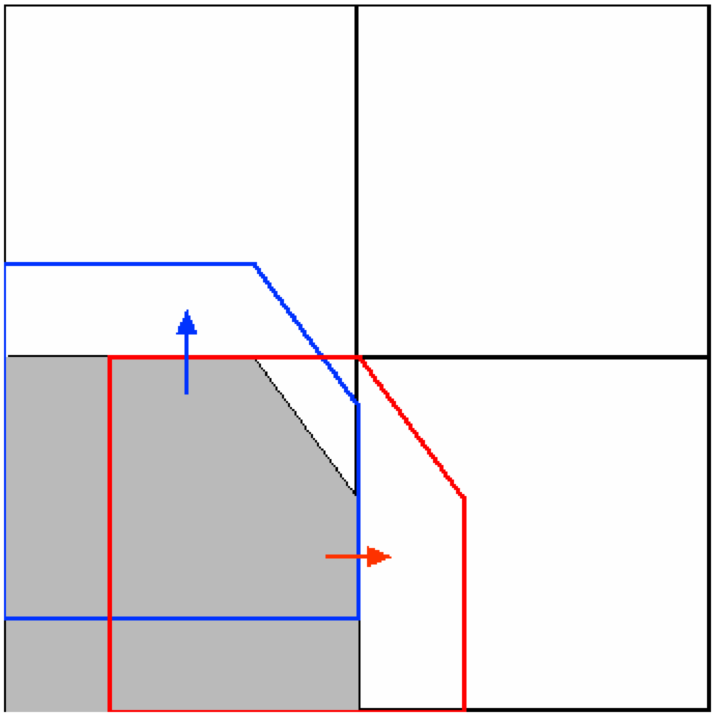

## Naive method

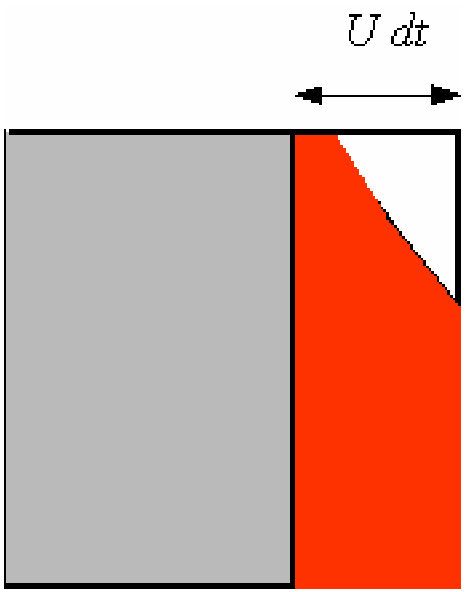


Geometrical definition of the discrete flux $\phi_x^n$

This is the « Eulerian » method. (as opposed to « Lagrangian »)

# Naive method

Problems:

•There is no propagation into the diagonal cell: the method fails trivially for a uniform velocity field and straight interface.

•There is no guarantee that after the two steps the result is bracketed between 0 and 1 ( $0 < C < 1$) . Without this, when $C > 1$, one has to resort to arbitrary removal of mass.

# ALTERNATING DIRECTIONS METHOD

The new method alternates directions. Here, first x-propagation the y-propagation

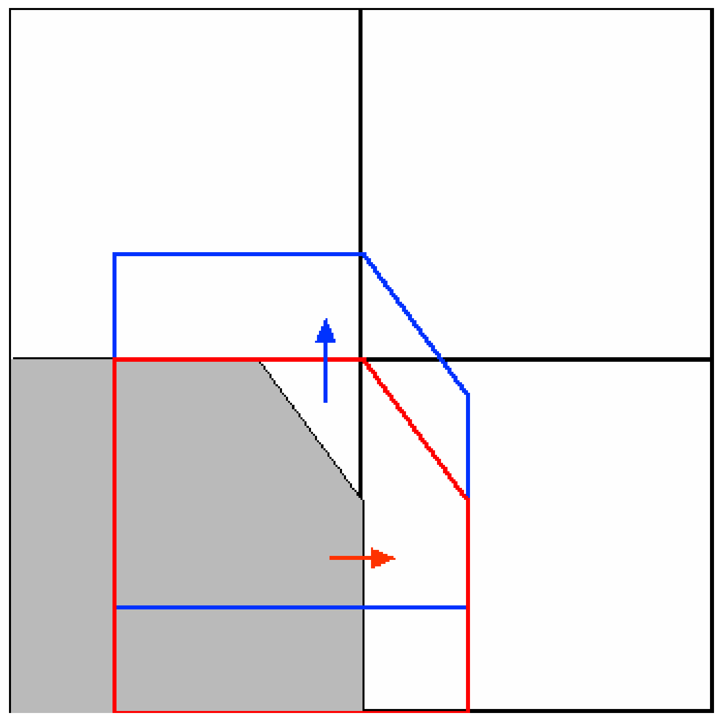

# ALTERNATING DIRECTIONS METHOD

1)

$$\frac{C_{ij}^{\ n+1/2} - C_{ij}^{\ n}}{\tau} = -D_x(u_x C^n)$$

2)

$$\frac{C_{ij}^{\ n+1} - C_{ij}^{\ n+1/2}}{\tau} = -D_y(u_y C^{n+1/2})$$

Does not preserve $0 < C < 1$.

# Kothe/Rider propagation method

1) Eulerian Implicit step

$$\frac{C_{ij}^{\,n+1/2} - C_{ij}^{\,n}}{\tau} = -D_x(u_x C^n) - (D_x u_x) C_{ij}^{\,n+1/2}$$

2) Explicit step

$$\frac{C_{ij}^{\,n+1} - C_{ij}^{\,n+1/2}}{\tau} = -D_y^*(u_y C^{n+1/2}) - (D_y u_y) C_{ij}^{\,n+1/2}$$

Leads to better mass conservation Does not preserve 0 < C < 1.

# AREA PRESERVING MAPPING

Lagrangian explicit + eulerian implicit is an *area-preserving* linear mapping of the plane!

$$x \to ax + b$$

$$y \to cy + d$$

where the Jacobian of the transformation is $J = ac = 1$.

# AREA PRESERVING MAPPING

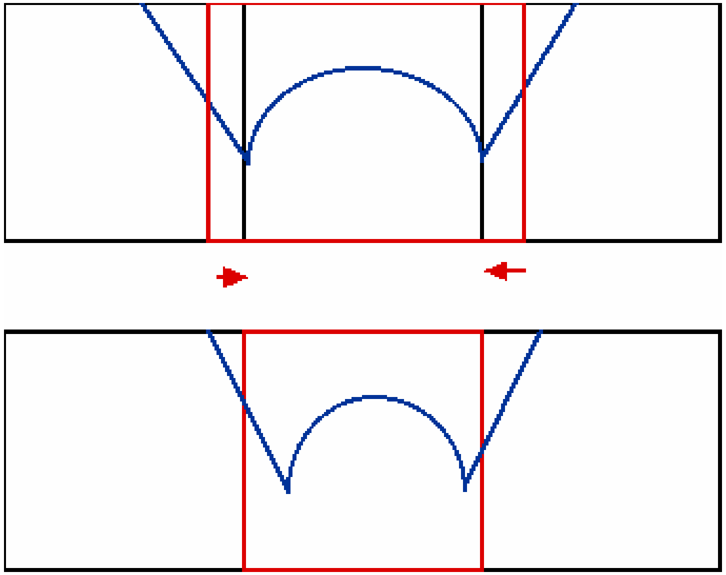

The first transform maps the top red rectangle on the bottom red rectangle. The velocities of the edges are node velocities.

# AREA PRESERVING MAPPING

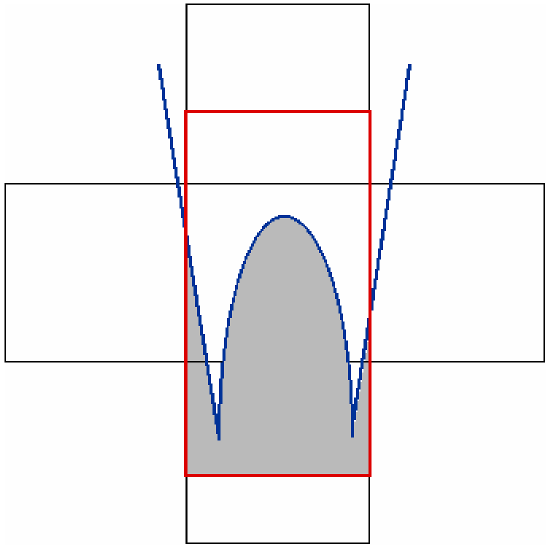

Lagrangian explicit propagation transforms the central square into the red rectangle. The original figure is stretched like Arnold 's cat, but its area is preserved. Moreover, the volume fraction remains $0 < C < 1$ since all steps are now geometrical transformations, and all areas may be computed explicitly.

Defects of VOF methods:

-- flotsam and jetsam (1960)
-- wisps (1990)
-- no defect (2003)

# TESTS

(a)

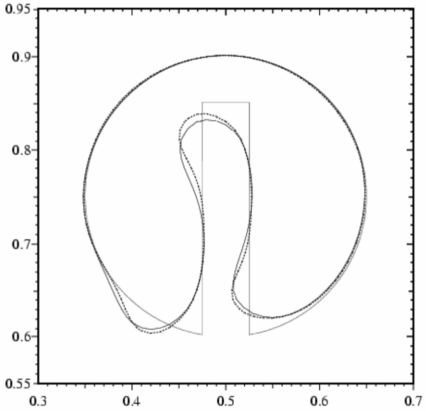


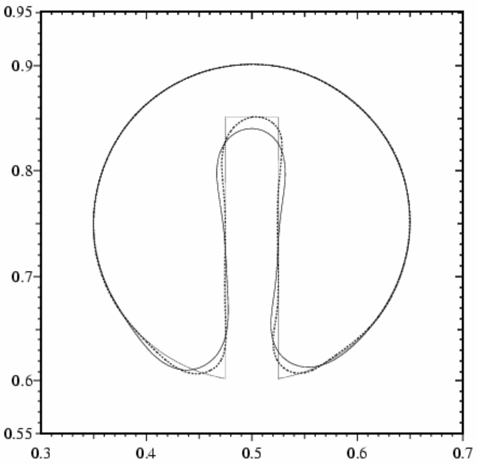


(b)

Zalesak 's test after ten solid body rotations. 100 x 100 grid
(a) ELVIRA (solid) and linear fit (dashed) reconstructions
(b) quadratic (solid) and quadratic with continuity (dashed).
Rotation is divergence-free, so all propagation methods give similar results.

# TESTS

Kothe and Rider’s spiralling, stretching and reversing flow.
Stream function:

$$\Psi = \sin^2(\pi x)\sin^2(\pi y)\cos\left(\frac{\pi t}{T}\right)$$

Naive propagation method

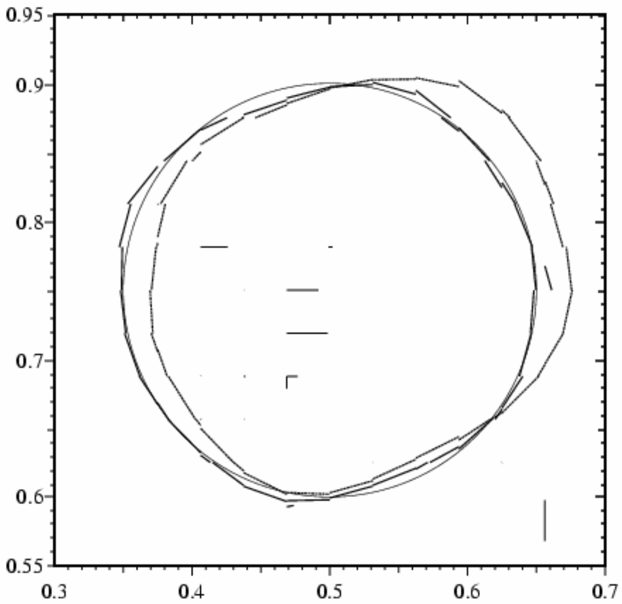


See wisps

New method with
various recontructions

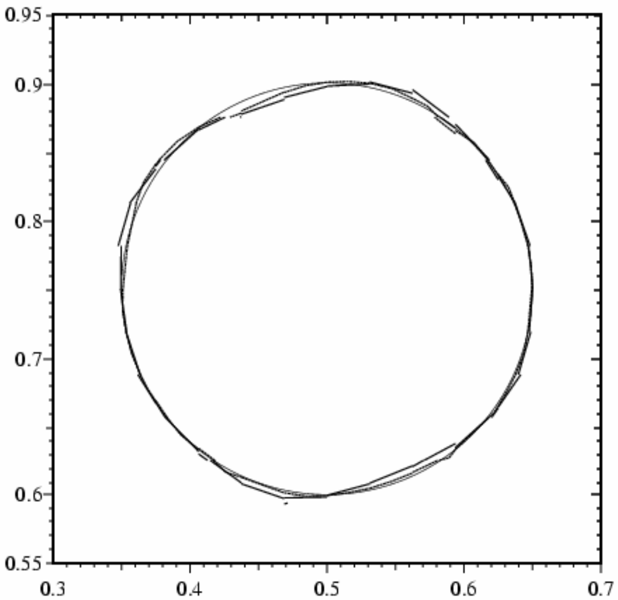


New developments: hybrid methods: VOF + LS,
markers + VOF, LS + markers.

# Method by Aulisa, Manservisi, Scardovelli (markers+VOF)

QuickTime™ et un
décompresseur Cinepak
sont requis pour visionner cette image.

# SURFACE TENSION

Treatment of surface tension by Continuous Surface Force
(« CSF » method, Brackbill, Kothe and Zemach JCP 1993)

$$\sigma\kappa\,\mathbf{n}\,\delta_S \approx \sigma\kappa^h\nabla^h C$$

Many methods for κ . Simplest:

$$\kappa = -\nabla\cdot\mathbf{n} \approx -\nabla^h\cdot\left(\frac{\nabla^h C}{\left|\nabla^h C\right|}\right)$$

# SURFACE TENSION

It is necessary to smooth the C function

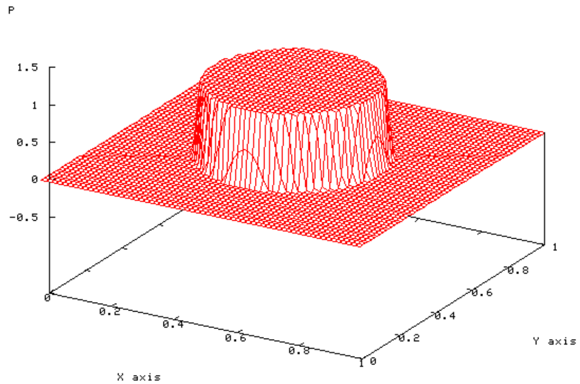


Raw C function

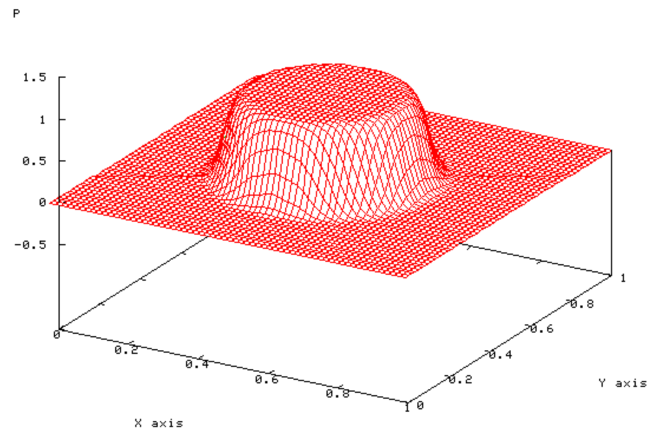


Filtered C function

# SURFACE TENSION

Elementary smoothing:

$$\tilde{C}_{ij} = \frac{1}{2} C_{ij} + \frac{1}{8}\left( C_{i+1,j} + C_{i-1,j} + C_{i,j+1} + C_{i,j-1} \right)$$

Kernel smoothing:

$$\tilde{C}(\mathbf{x}) = \int C(\mathbf{y}) K_{\varepsilon}(\|\mathbf{x} - \mathbf{y}\|) d\mathbf{y}$$

# SURFACE TENSION

Typical kernel

$$K_\varepsilon(r) = A(\varepsilon)\left(1-\frac{r^2}{\varepsilon^2}\right)^4 \qquad \text{for } r < \varepsilon$$

The constant A is chosen to normalize the discrete approximation.

# SURFACE TENSION

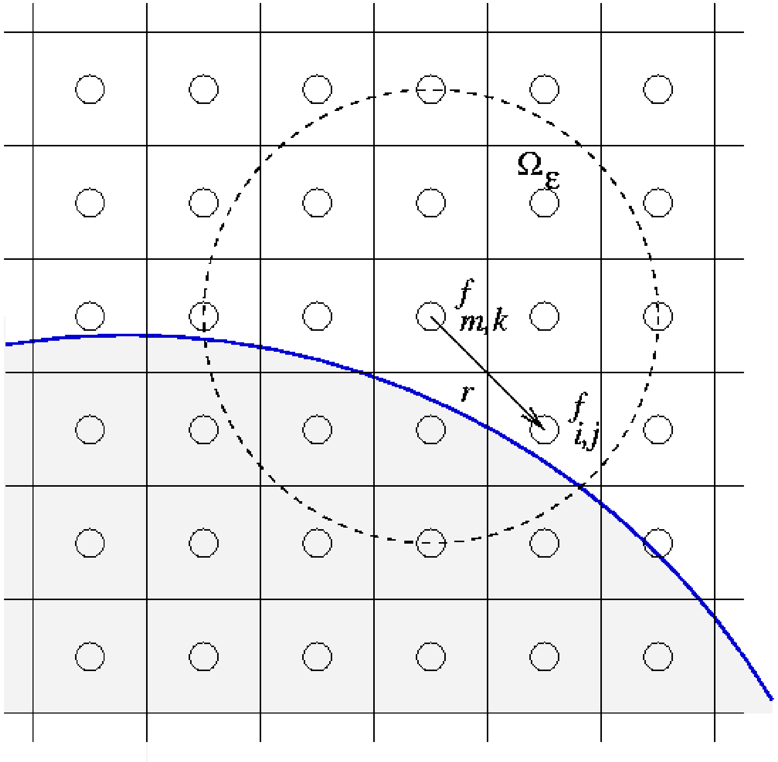


Discrete Kernel implementation

$$\tilde{C}_{ij} = \sum_{lm} K_\varepsilon(x_{ij} - x_{lm}) C_{lm}$$

# SURFACE TENSION

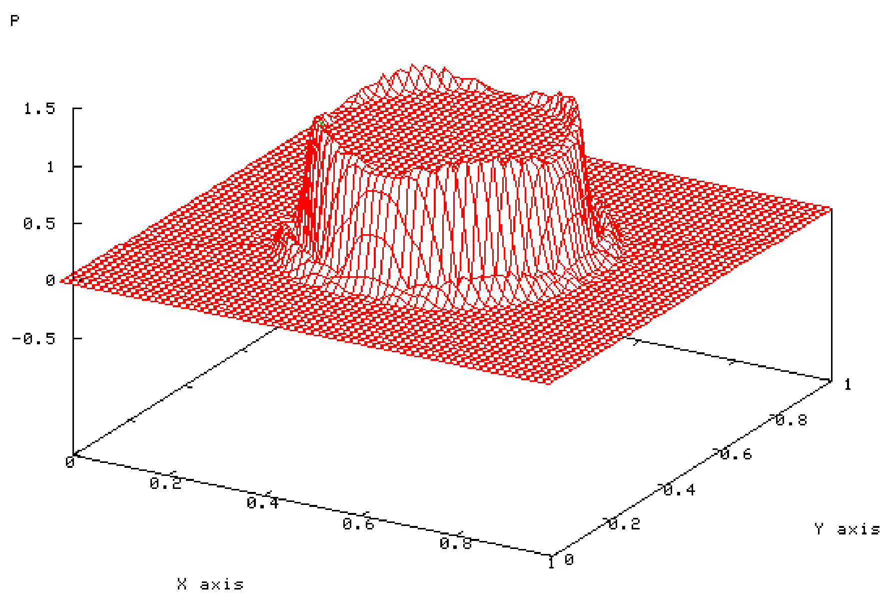


Verification of Laplace's law for a static bubble :

$$R\,\Delta P\,/\,\sigma\ = 1\ \ .$$

# SURFACE TENSION

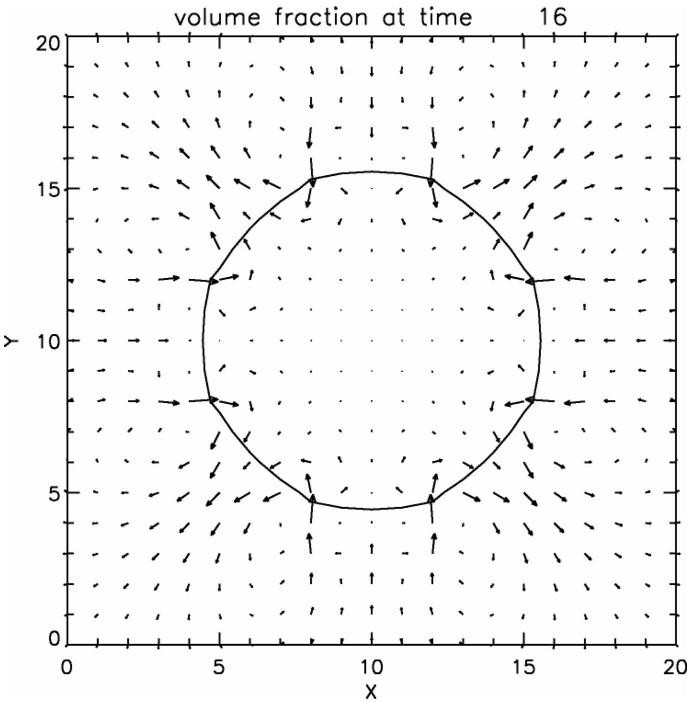


Spurious currents around a static bubble.

Leads to difficulties when there is both a large density ratio and a large surface tension as it is the case for air-water interfaces

# SURFACE TENSION

The spurious current problem arises because of the discontinuity of *p*. Similar problems arise because of the discontinuity of $\rho\mathbf{g}$ (when a free surface with gravity is not aligned with the grid), and also because of the discontinuity of $\mu\mathbf{D}$**.**

Cut cell methods attempt better approximation of the various balances inside the cell.

This requires the accurate knowledge of the position of B and E, which may be done by abandoning VOF and reverting to marker particles.

# SURFACE TENSION

markers chain : advect each marker.

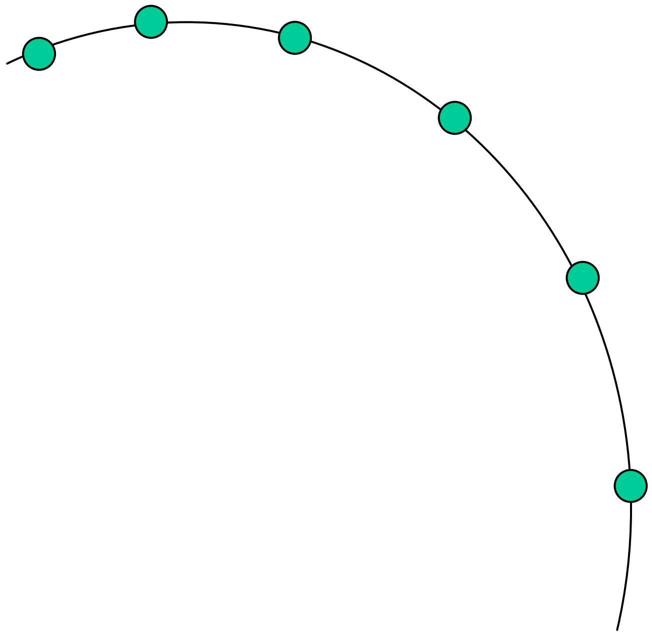

# SURFACE TENSION

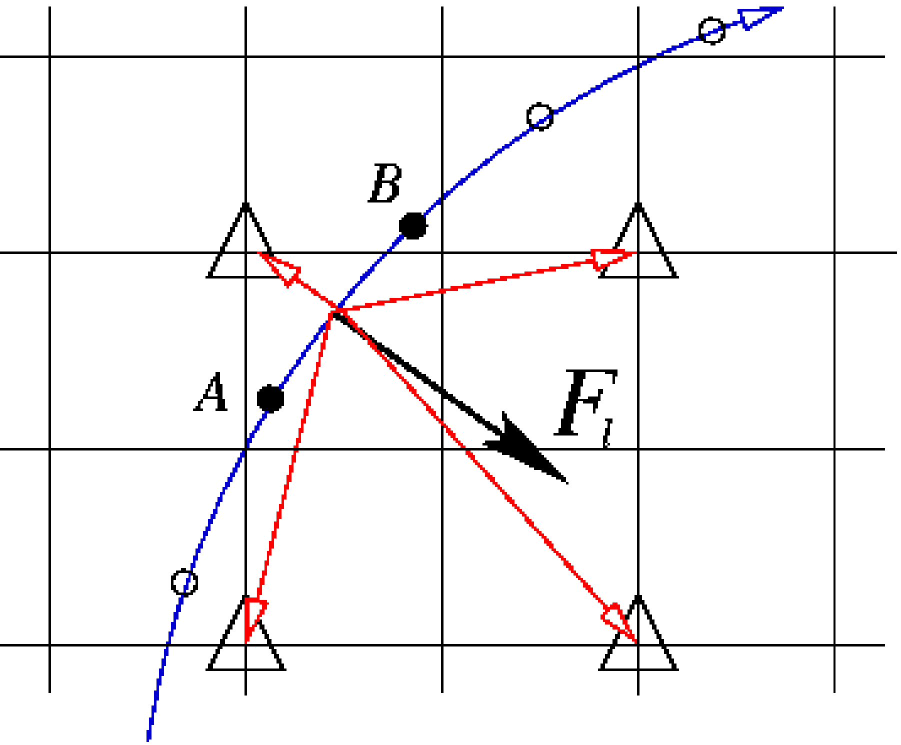


An elementary way to distribute the surface tension force on the grid (Tryggvason's method)

CUT CELL/MARKER METHODS

Another point of view involves looking at the momentum balance:

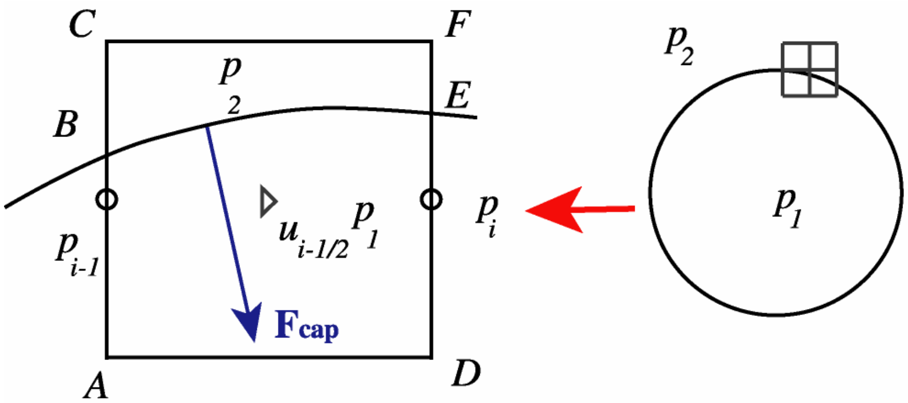


Exact balance equations:

$$p_1 - p_2 = \sigma / R$$

$$F_{cap} \cdot \mathbf{x} + \int_A^C p\, dl - \int_D^F p\, dl = 0$$

But if $p_i = p_{i-1}$ on figure then the discrete balance equation is not satisfied:

$$F_{cap} \cdot \mathbf{x} + p_i - p_{i-1} \neq 0$$

CUT CELL/MARKER METHODS

Cut cell methods try to improve the approximation of the momentum balance:

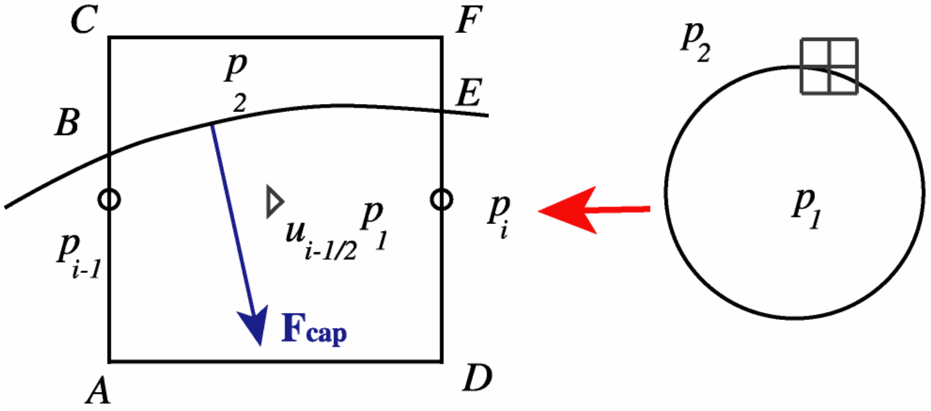


$$F_{cap} \cdot \mathbf{x} + \int_A^C p \; dl - \int_D^F p \; dl \approx F_{cap} \cdot \mathbf{x} + p_{i-1,j} AB + p_{i-1,j+1} BC + p_{i,j} DE + p_{i,j+1} EF$$

# CUT CELL/MARKER METHODS vs Level Set/VOF

Advantages:

- great accuracy
- control when reconnection occurs

Drawbacks

- complex to code in 3D (use computational geometry?).
- no automatic reconnection
- no exact mass conservation.

## VISCOSITY AND DENSITY

Viscosity and density jumps are treated by averaging in mixed cells of volume fraction $0<C<1$. The arithmetic mean is

$$\mu = C\mu_1 + (1-C)\mu_2$$

The harmonic mean is

$$\frac{1}{\mu} = \frac{C}{\mu_1} + \frac{1-C}{\mu_2}$$

Which mean is better depends on flow geometry

# VALIDATION OF VOF/MARKER METHODS

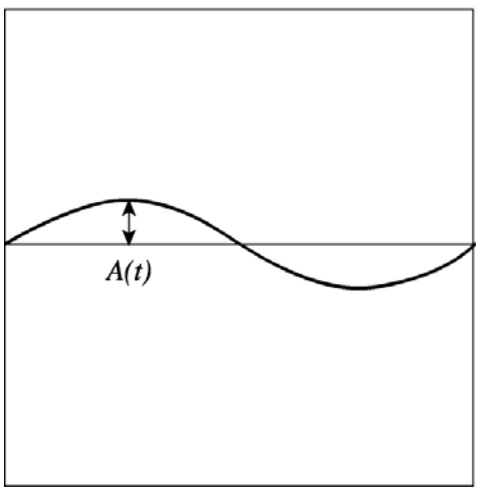


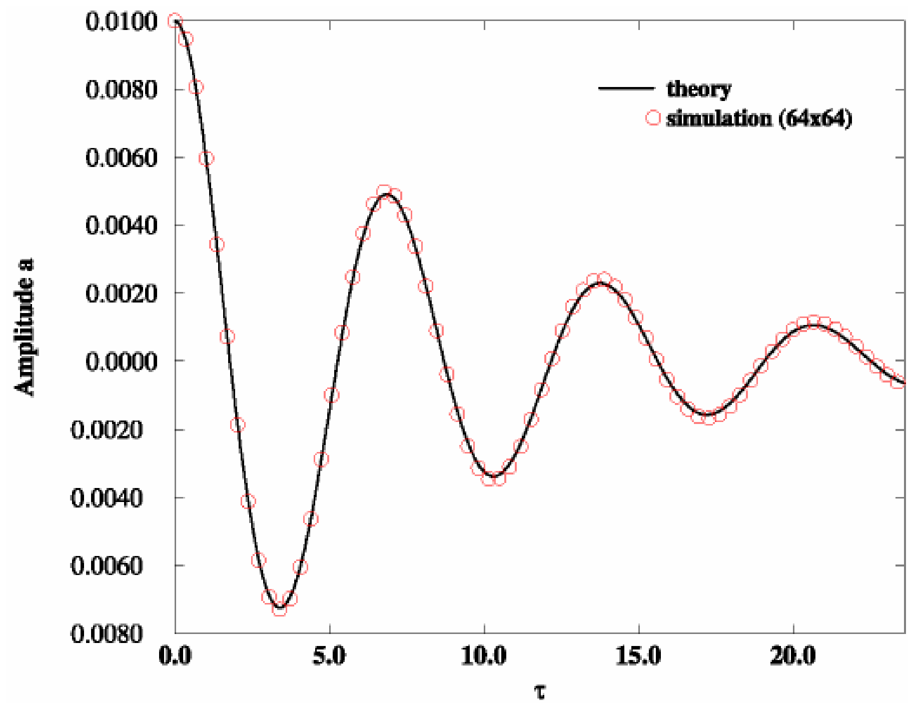


Comparison of analytical and numerical solutions for capillary waves, box size 64 x 64 VOF method.

# VALIDATION

Mode 2 oscillation of a bubble (marker cut-cell method)

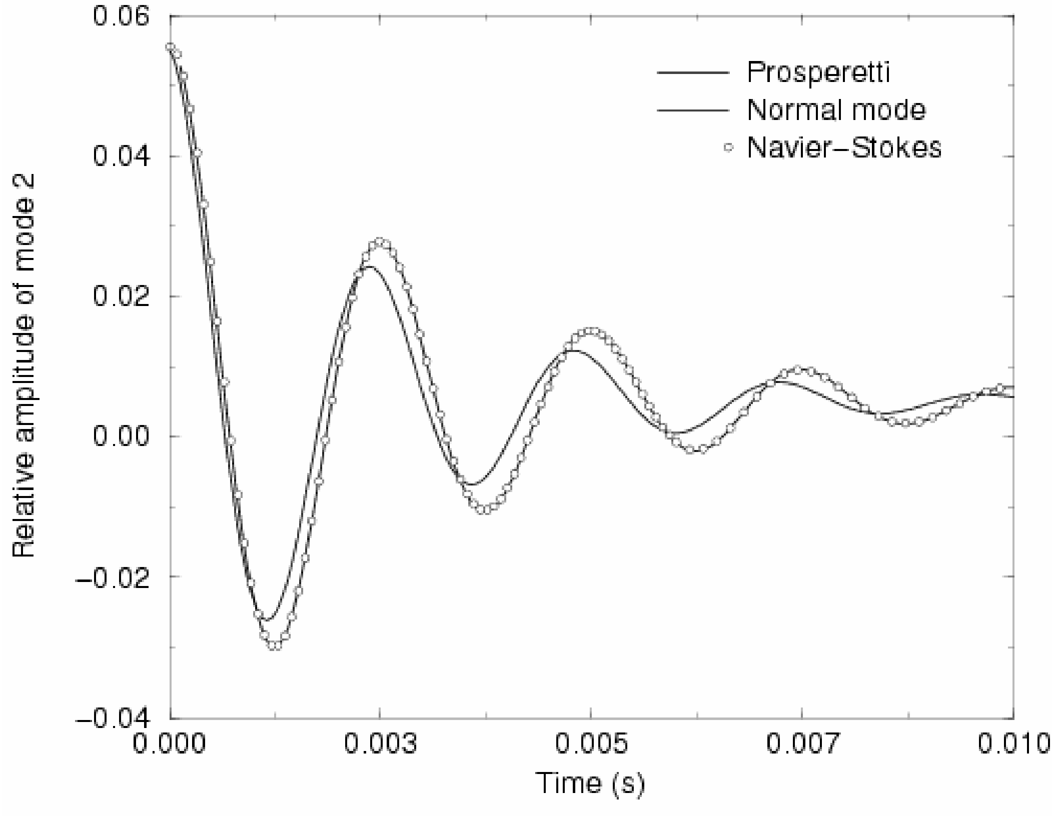

# VALIDATION

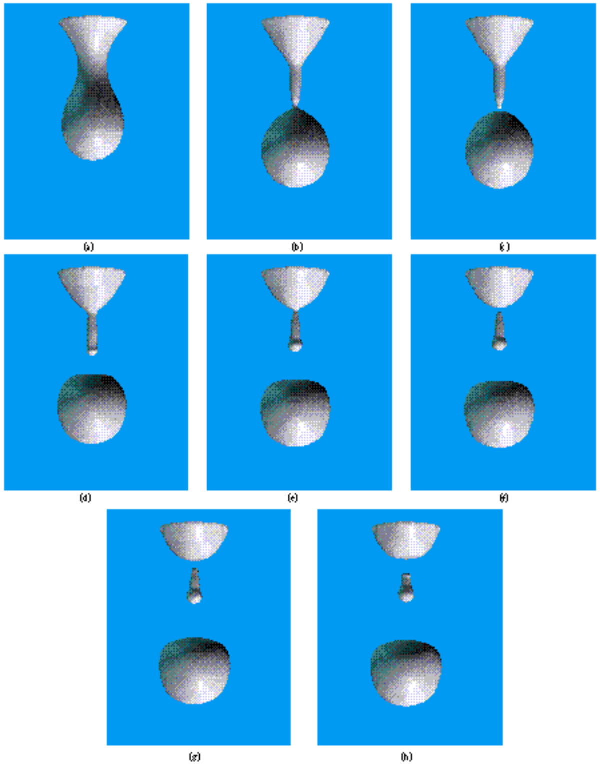


Reconnection (VOF, by Denis Gueyffier)

# VALIDATION

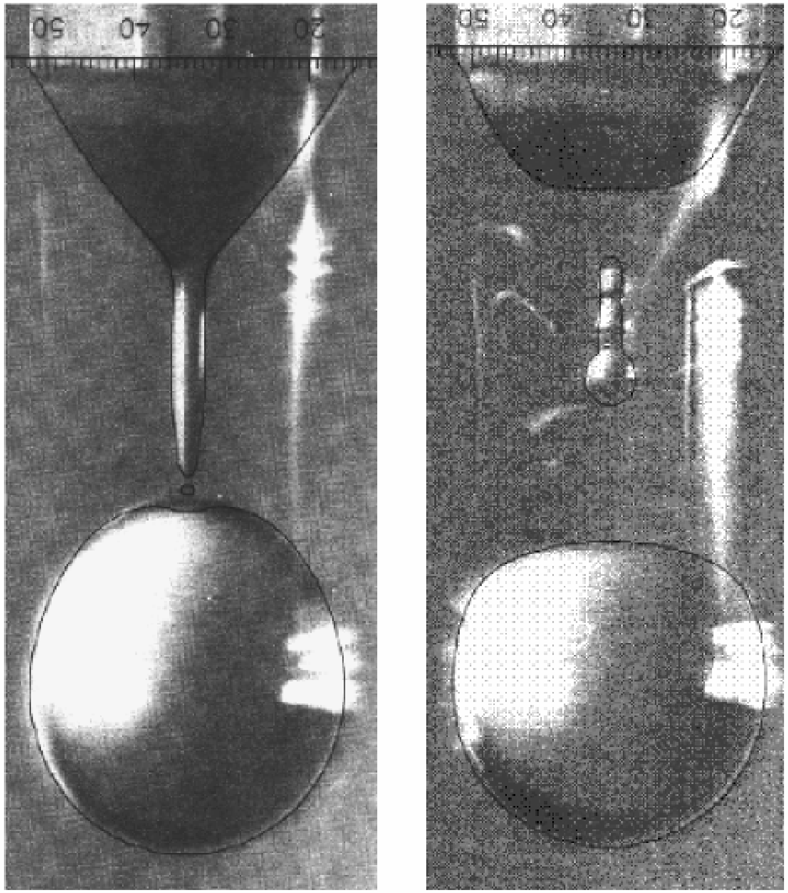


Experiment by Peregrine.

Simulation: VOF method, D. Gueyffier

# VALIDATION

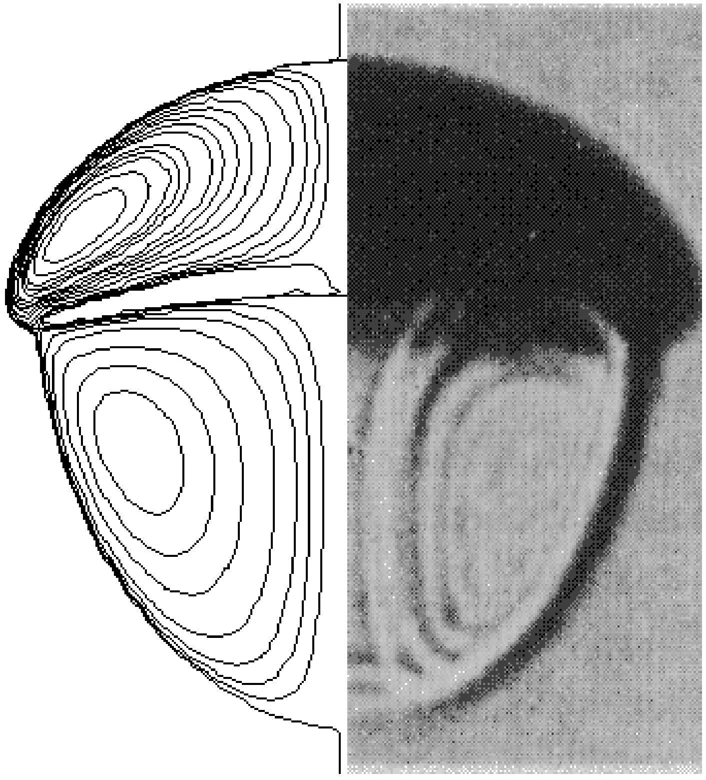

Right: rising bubble in oil, experiment.

Left: Simulation using the VOF method

# VALIDATION

## Kelvin-Helmholtz instability

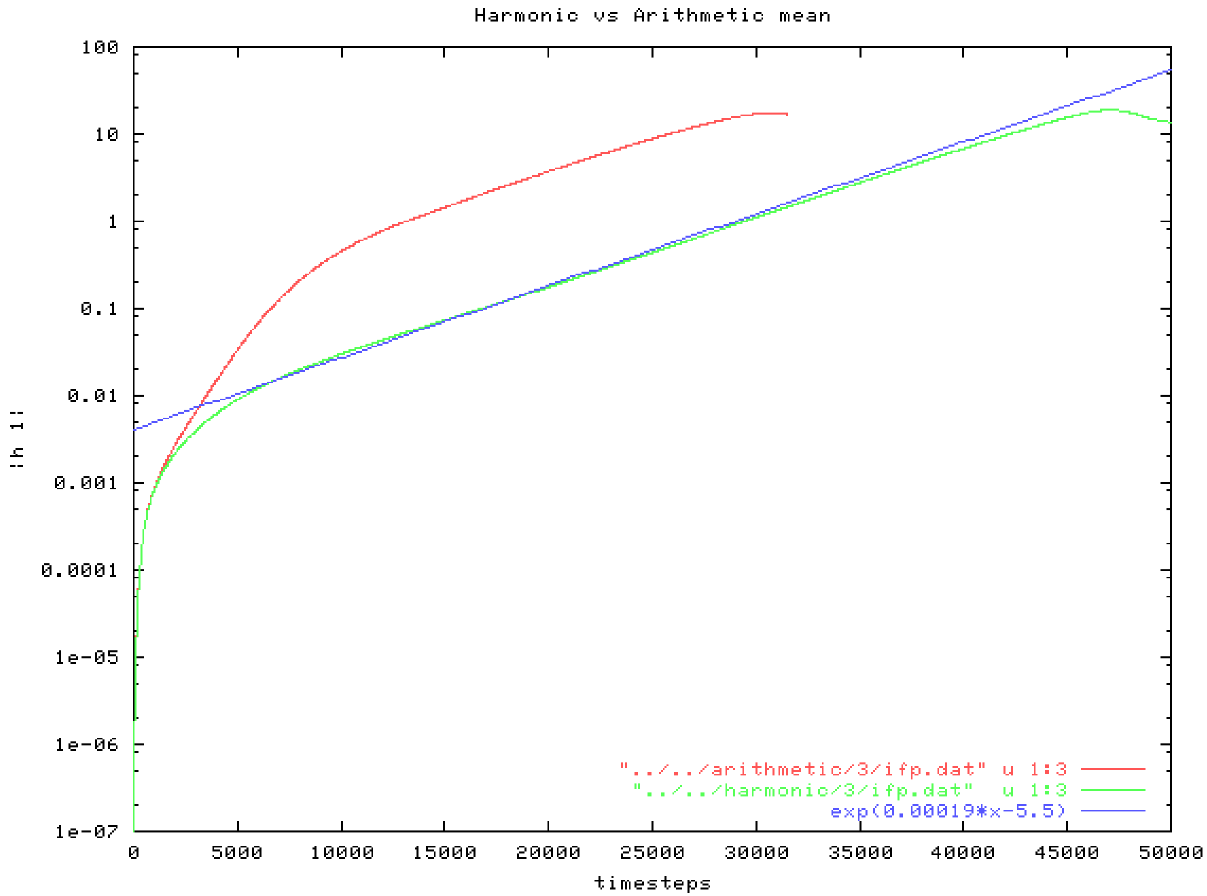


Code/linear theory comparison

Better to use harmonic mean of viscosity in mixed cells (green curve)

# WHAT CAN THIS BE USED FOR ?

- Atomization
- Droplet impact
- Cavitation bubbles
- Bursting bubbles

# ATOMIZATION

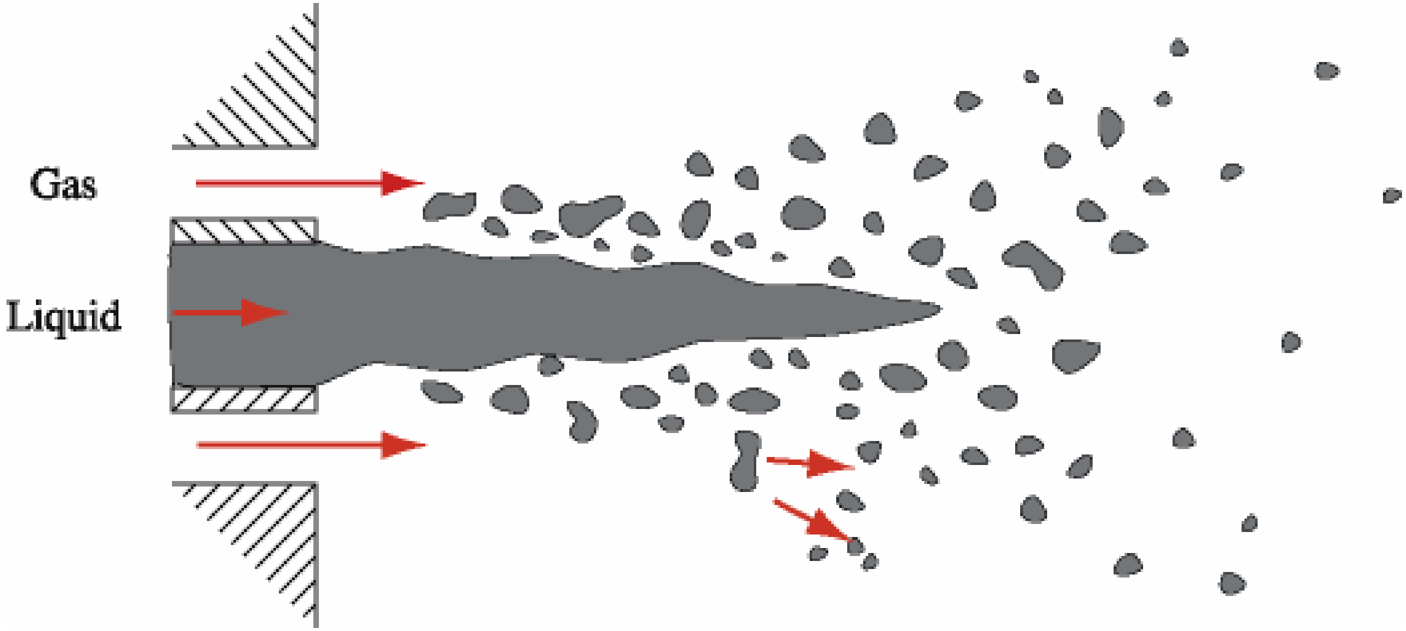


Coflowing jet atomization. Standard representation.

# ATOMIZATION

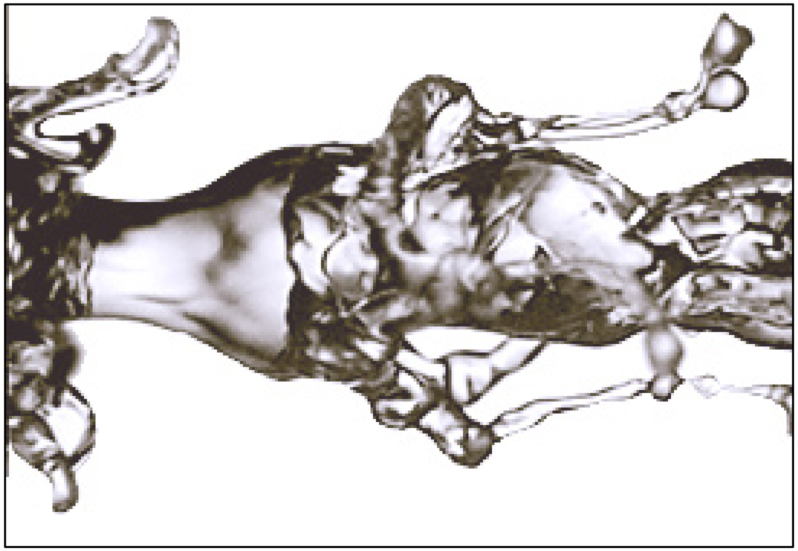

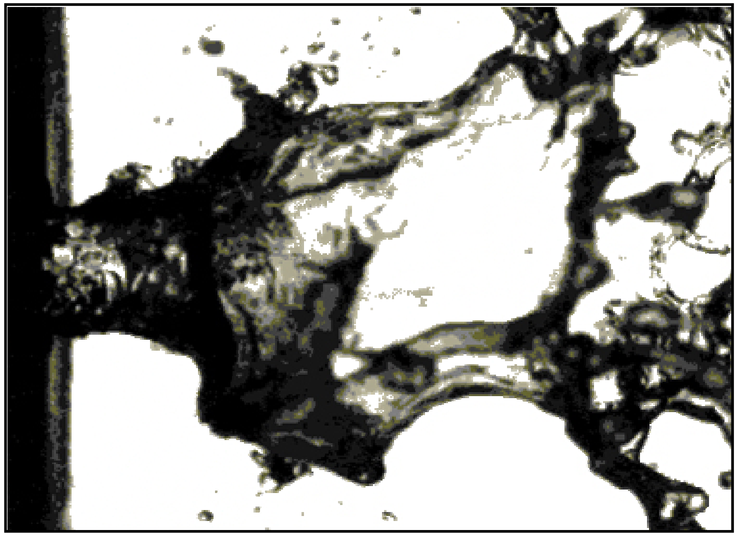

Lasheras, Hopfinger,Villermaux, Raynal, Cartellier …, (San Diego, Grenoble and Marseille)

# ATOMISATION

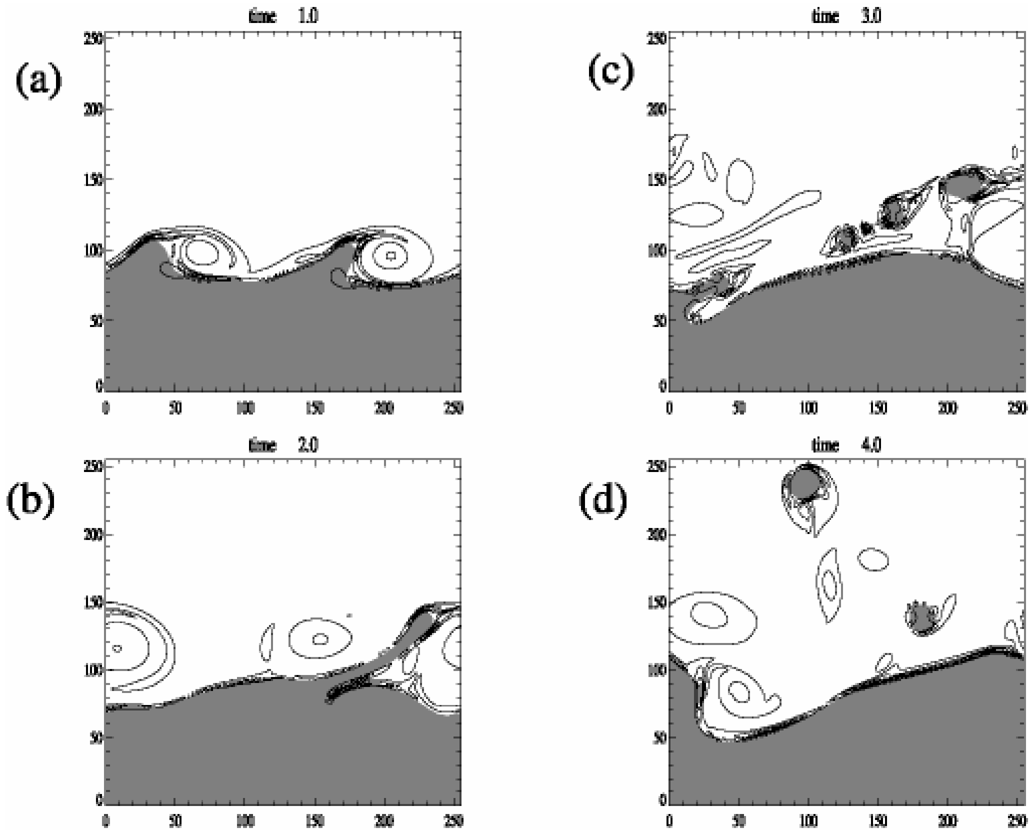


Droplet deformation in a 2D shear layer.

Diesel engine (no coaxial gas flow)

Entry and exit conditions.

$V_{inj} = 300\ m.s^{-1}$

$r_{inj} = 0.1$ mm

$\rho_{gaz} = 20\ kg.m^{-3}$

2 x 8 mm

(1024 x 4096)

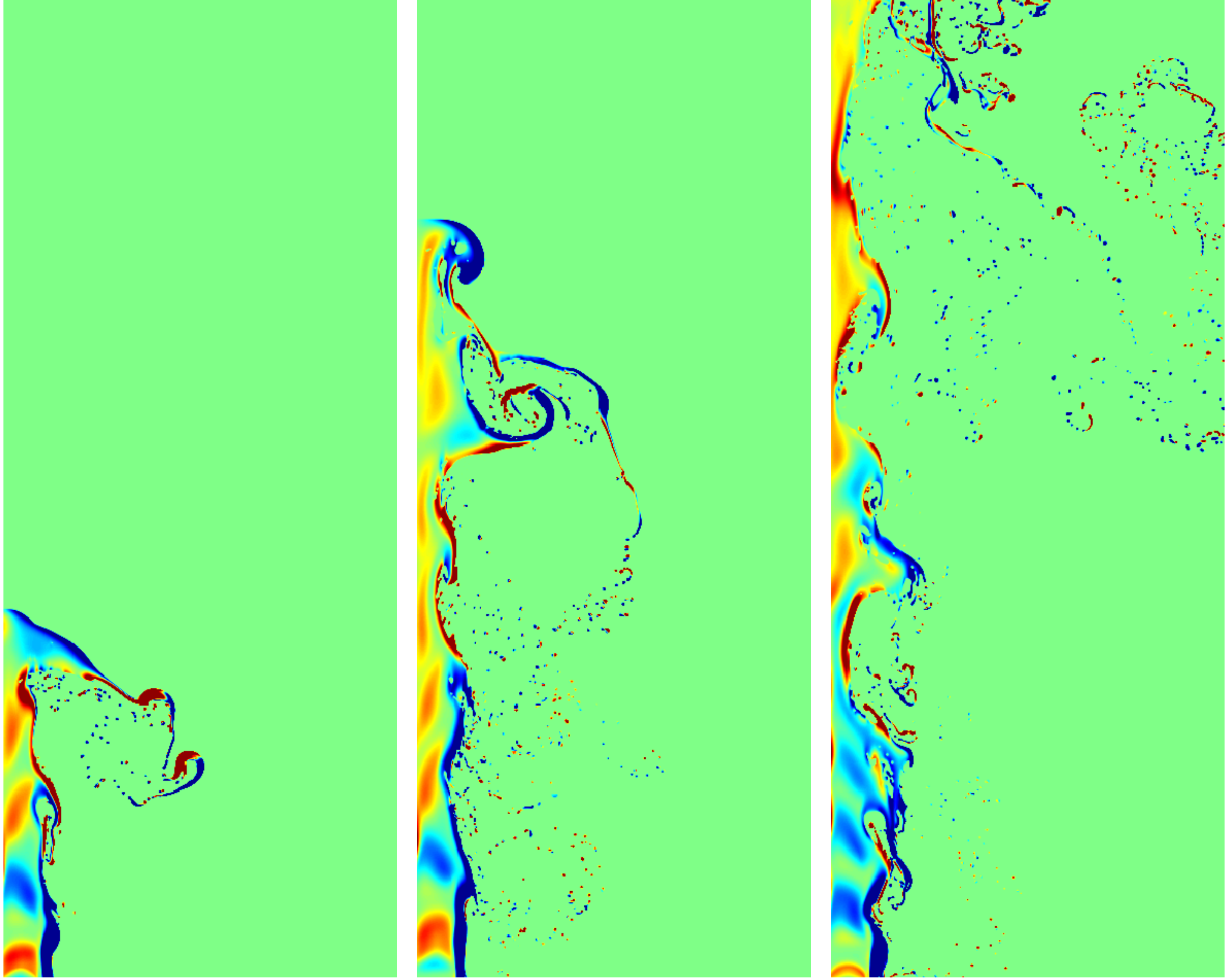

Laminar flow upstream

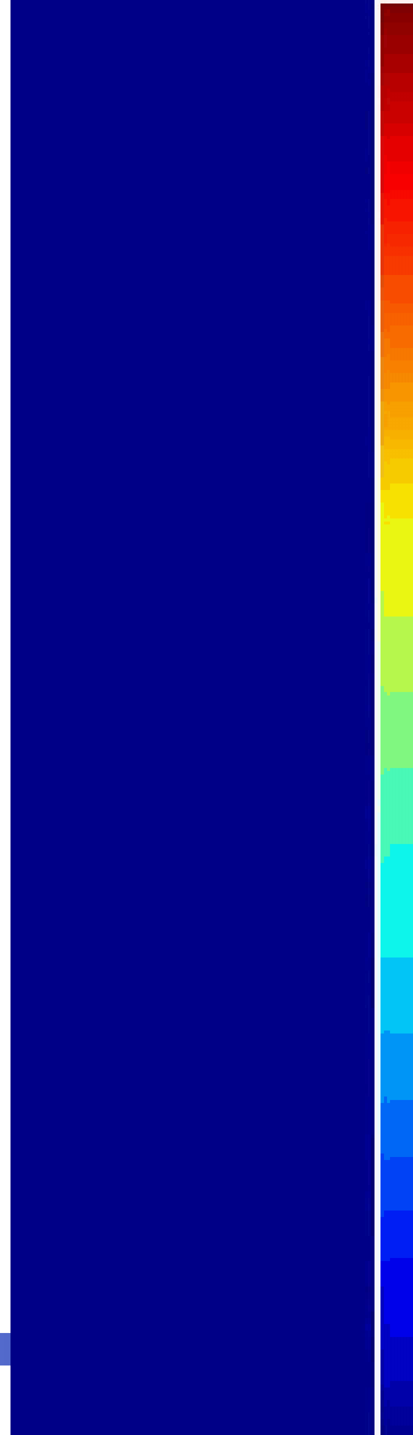

With upstream "turbulence"

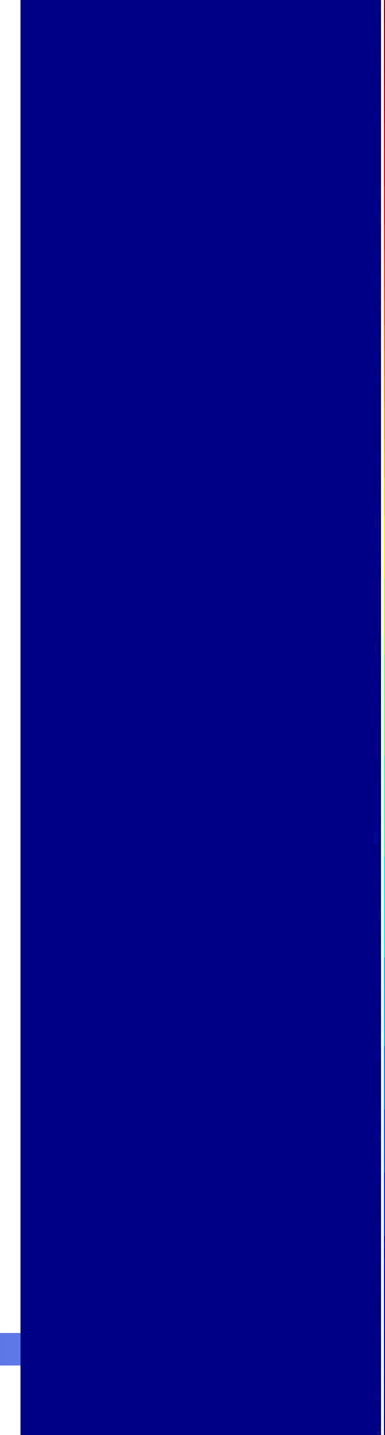

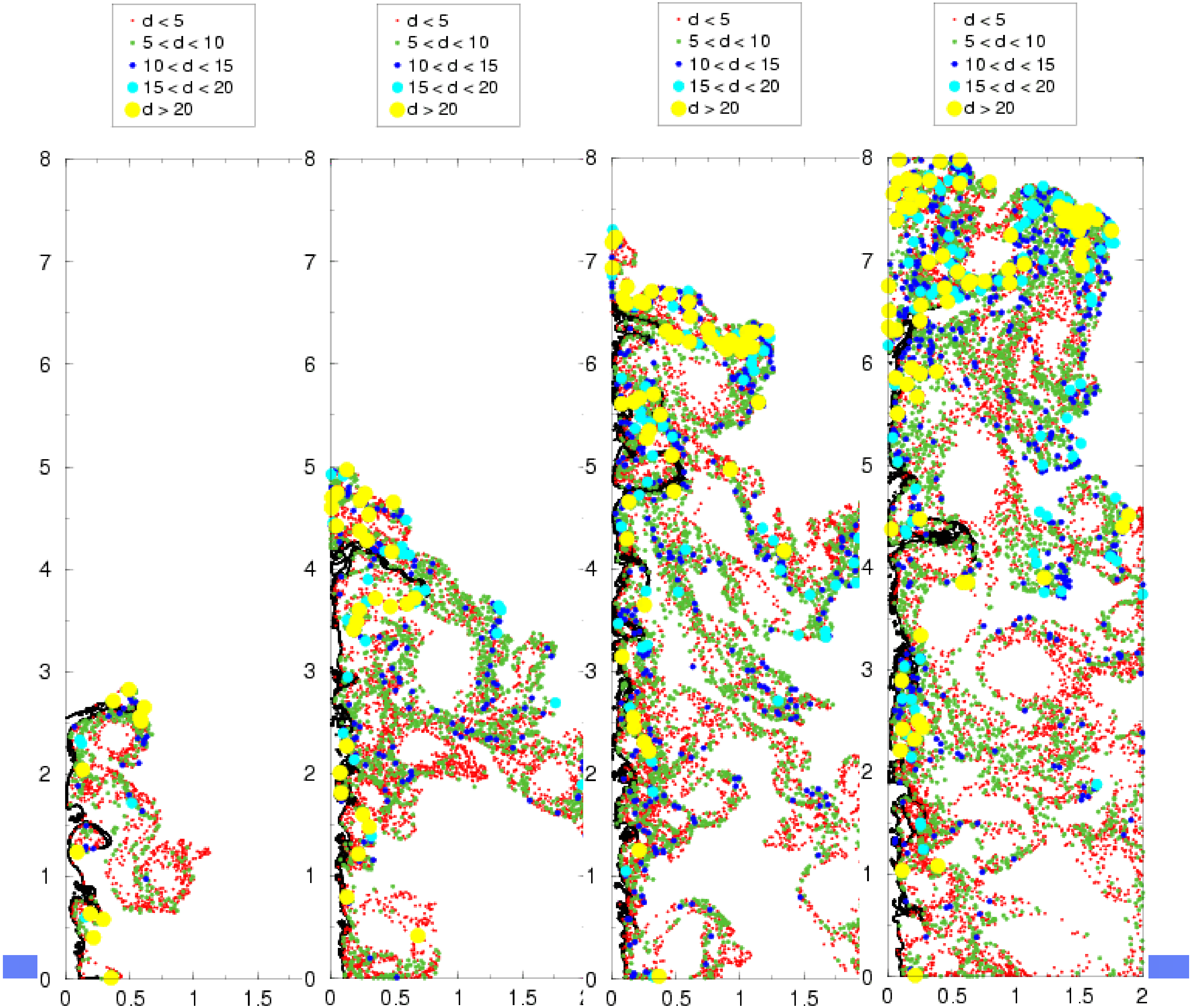

d < 5
5 < d < 10
10 < d < 15
15 < d < 20
d > 20
0
0.5
1
1.5
2
0
1
2
3
4
5
6
7
8

# ATOMISATION

## Co-flowing atomizer

Parameters:

- 512 x 1024 grid
- $r_L = 20$ kg / m$^3$
- $r_G = 2$ kg / m$^3$
- $U_G = 100$ m/s
- M = 2.5

- R = 400 microns
- $\mu_L = 0.002$ kg/m/s
- $\mu_G = 0.0001$ kg/m/s
- $U_L = 20$ m/s
- $\sigma = 0.030$ kg/s$^2$

# ATOMISATION

Same with turbulent entry (Enrique Lopes-Pages)

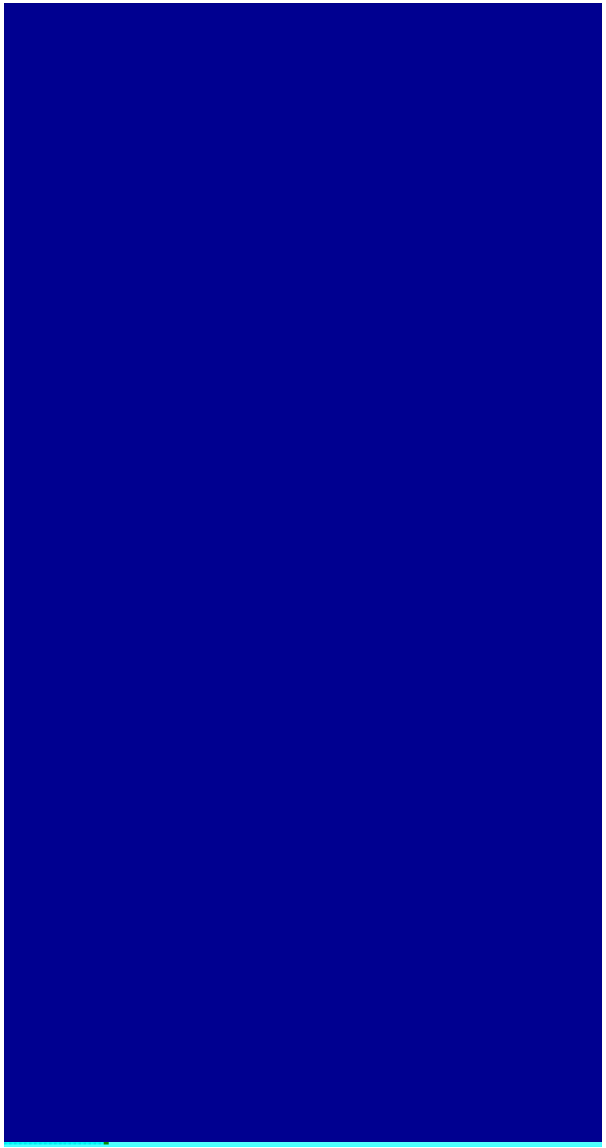

# Droplets' distribution function in coaxial jets

Laminar

Turbulent

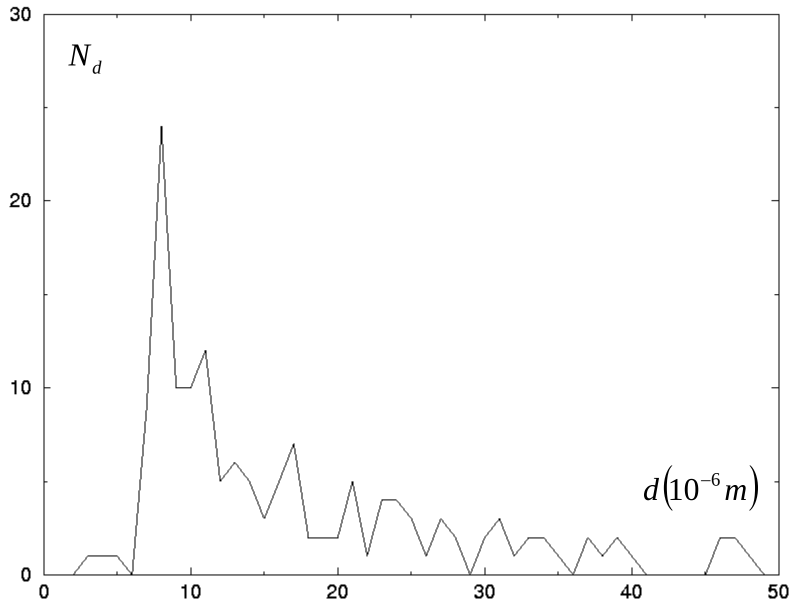


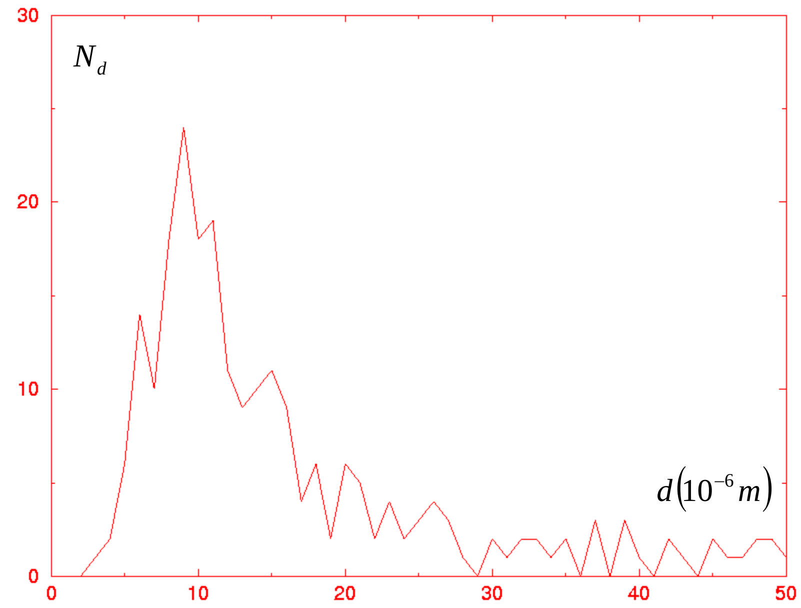

$128^3$ simulations

3D VOF code, space periodic simulation. Diesel engine conditions.

A rare event:
Breakup after sheet puncturing

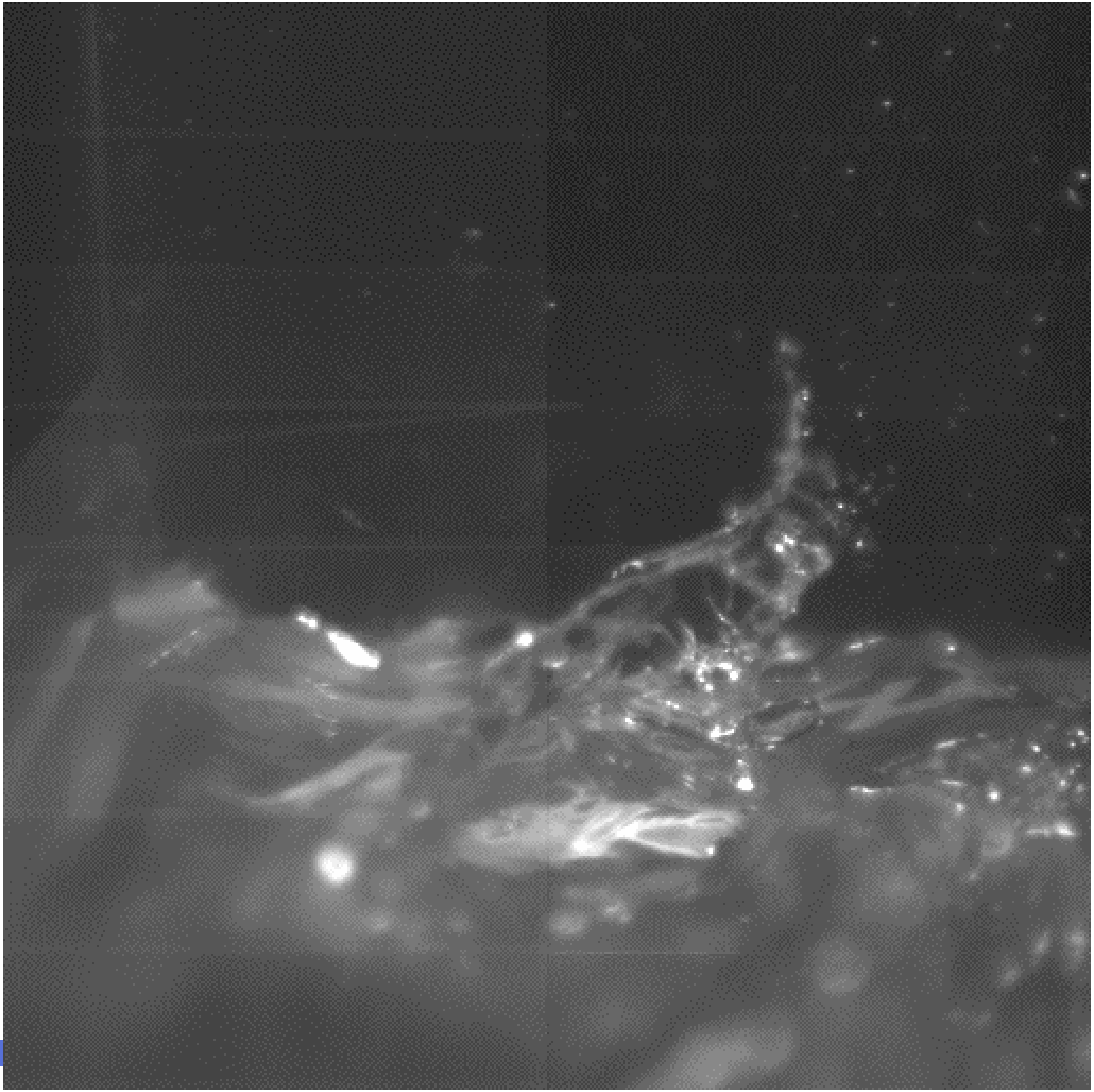

Show movie

- 256x128x128 (2x1x1 mm) (16 procs 16x128x128 - 1 week)
- injection : 200 m/s
- t step : 0.25 ns
- density ratio diesel/air : 8.5

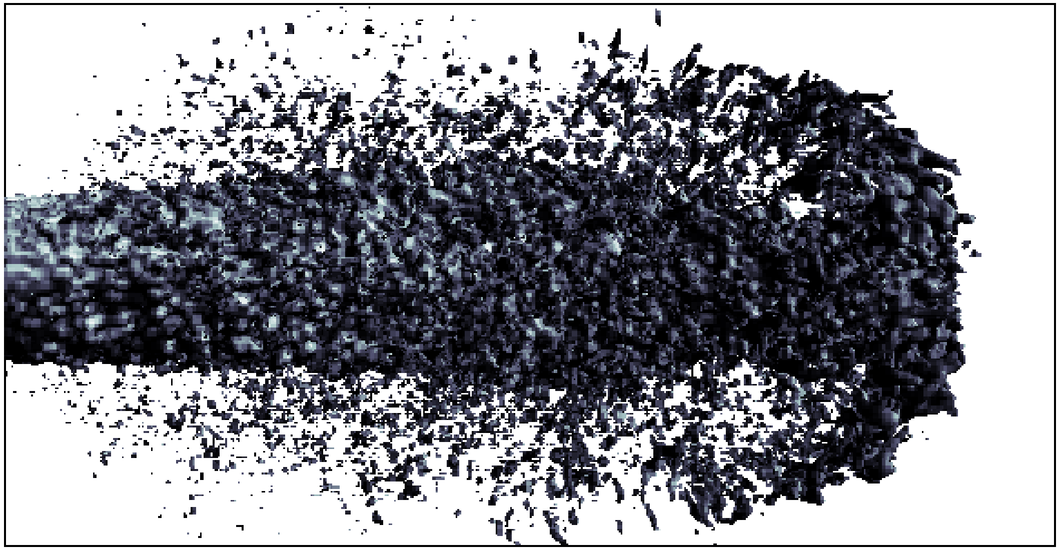

3D
(Anthony
Leboisssetier)

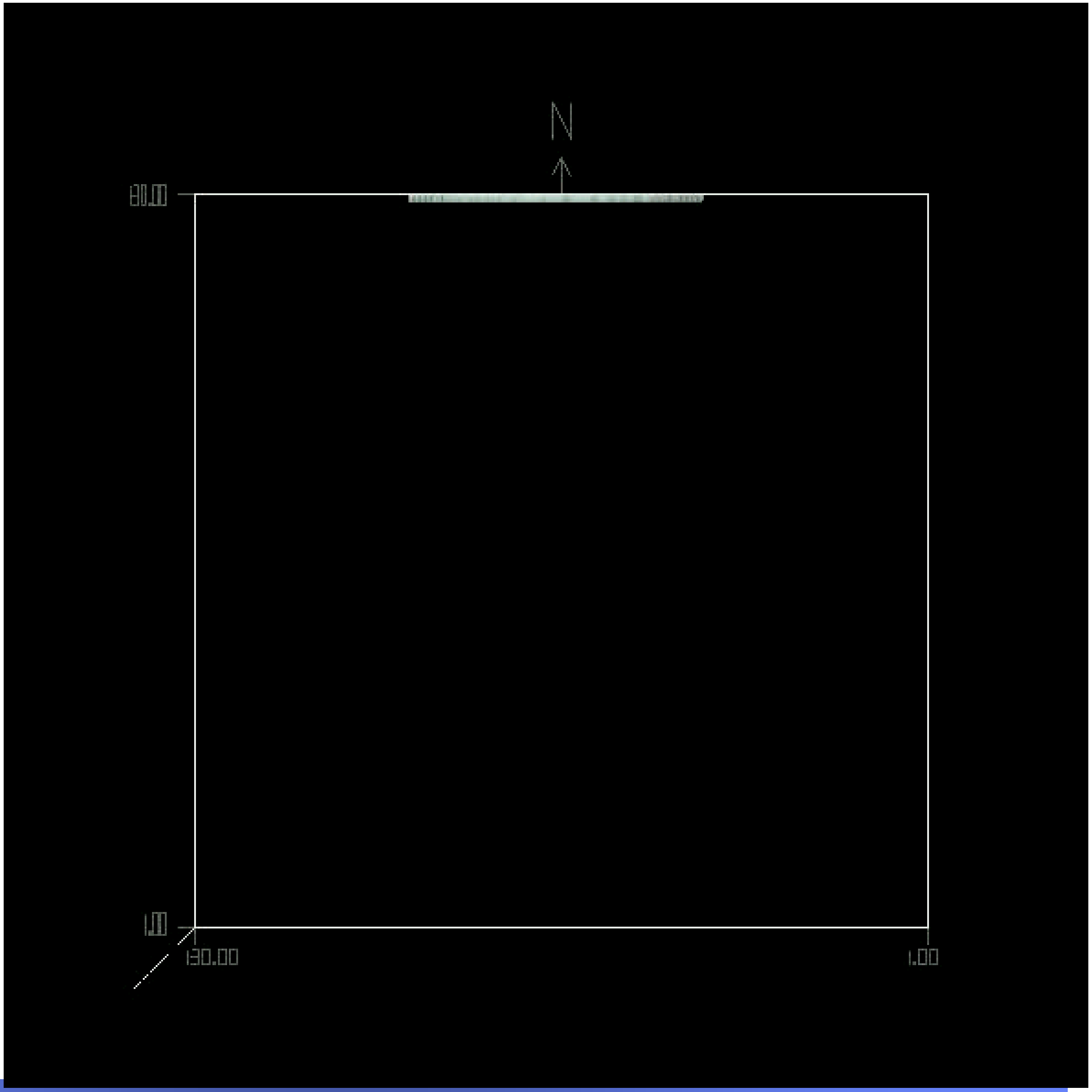

# Conclusions

Comparaison with linear theory validates the code.

- The turbulence level on entry is important.
- Droplet sizes are exponentially distributed.
- A 2D mechanism for filament formation was found.
- Still debate on the 3D mechanism

# Forecast

Present simulations in spatial 2D are resolved up to 512 x 2048. An equivalent resolution in 3D requires 512 x 512 x 2048 simulations. One can perform 128 x 128 x 256 on a 16-proc. PIII cluster. An additional factor of about 128 in CPU is necessary.

-It is likely that the 3D problem will be sufficiently resolved circa 2010.

-This forecast was published in 2001 (Scardovelli and SZ) and at the same time it was predicted that the droplet splashing problem would be solved in 2005 … well let us see.

# DROPLET IMPACT

Simulation setup

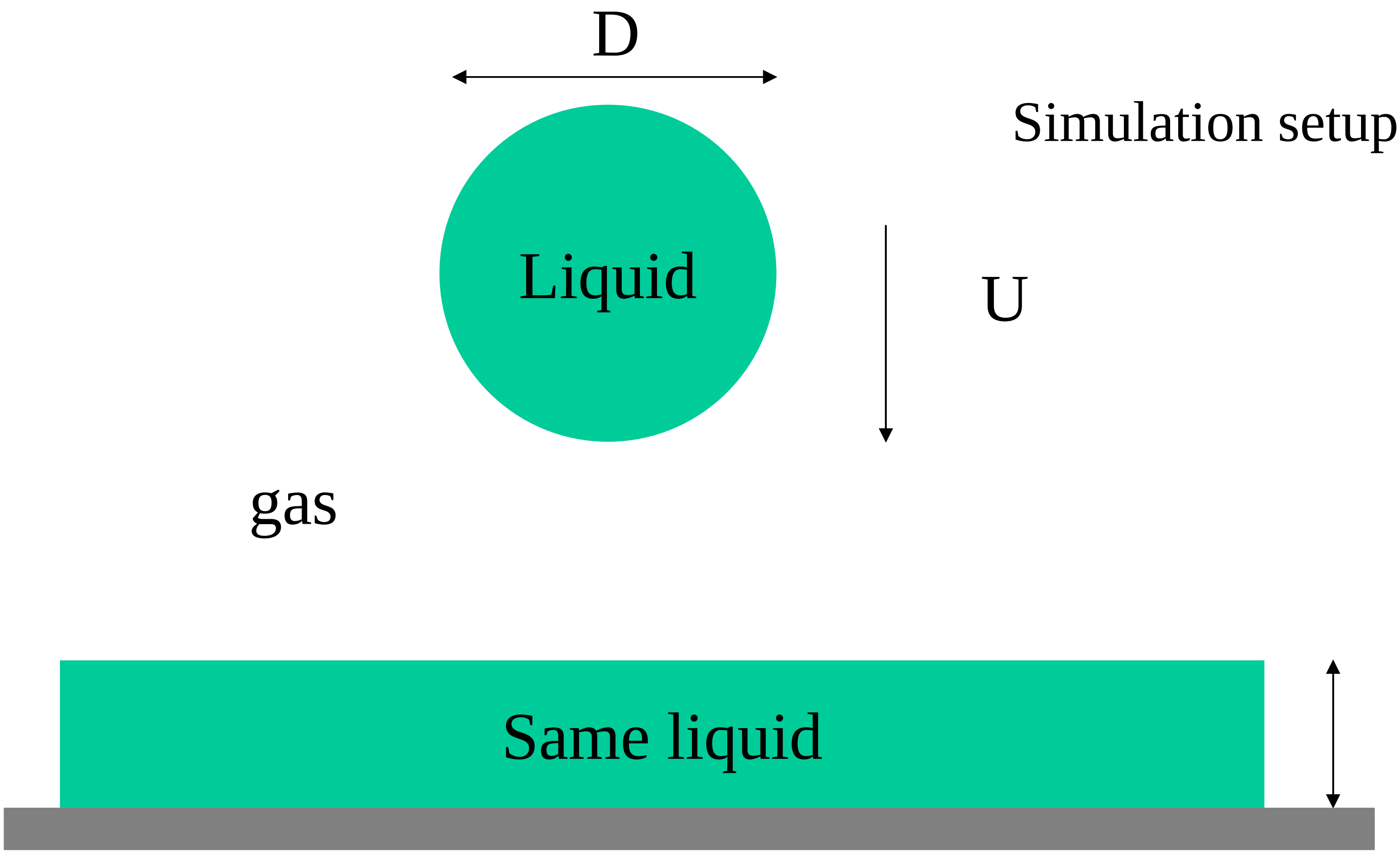

# DROPLET IMPACT

Early-forming jets are thin.

Perhaps an explanation to the prompt splash: (droplets break early on rough surfaces) phenomenon ?

Navier-Stokes equations, two phases.

Both liquid and gas are simulated.

Example: 2 mm glycerine droplet at 6m/s

Liquid and gas are incompressible.

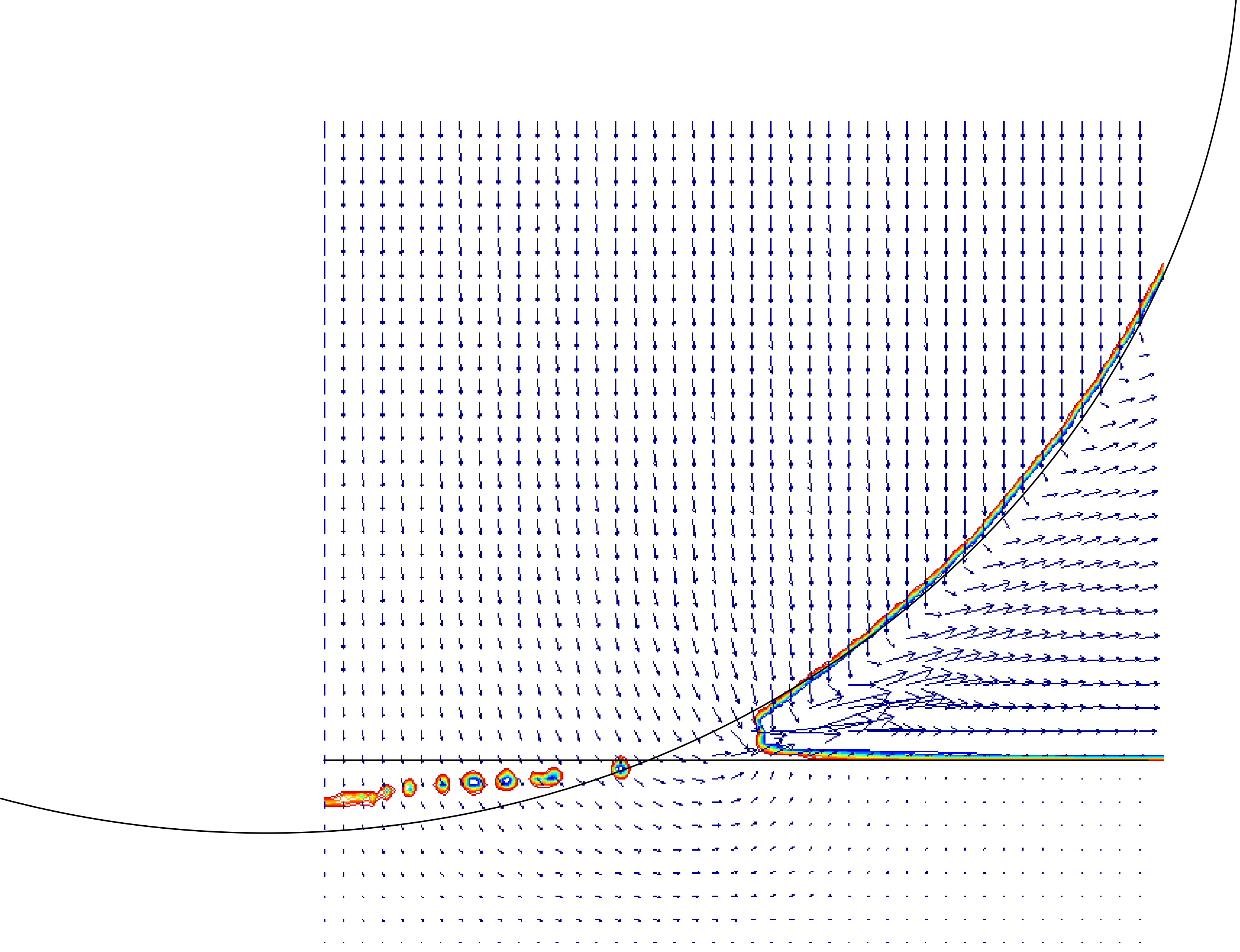

# DROPLET IMPACT

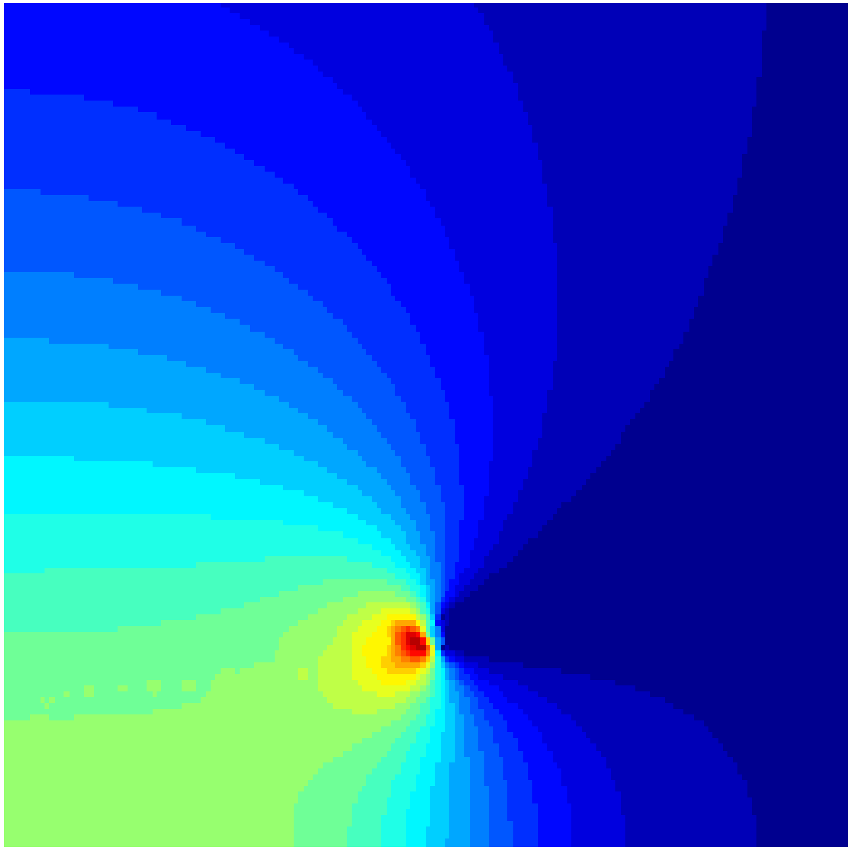

Pressure field

# DROPLET IMPACT

QuickTime™ et un
décompresseur Codec YUV420
sont requis pour visionner cette image.

Axisymmetric.

Low Re Case

Re=100
We=8000

QuickTime™ et un
décompresseur Codec YUV420
sont requis pour visionner cette image.

High Re Case

Re=1000

We=8000

# DROPLET IMPACT

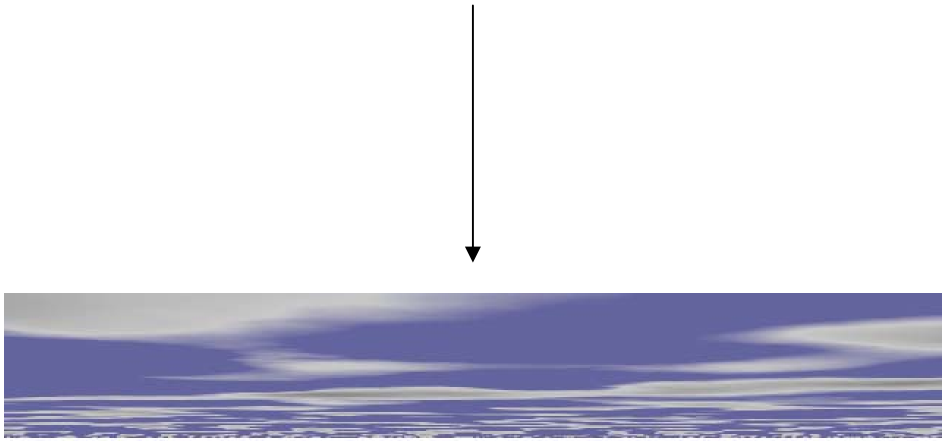

What happens in 3D ?

Look from above

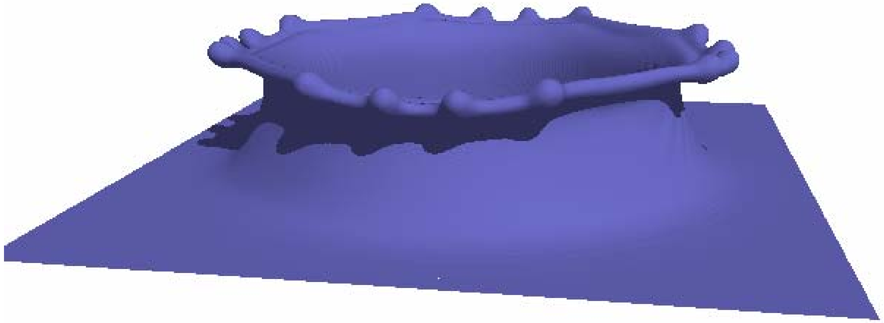

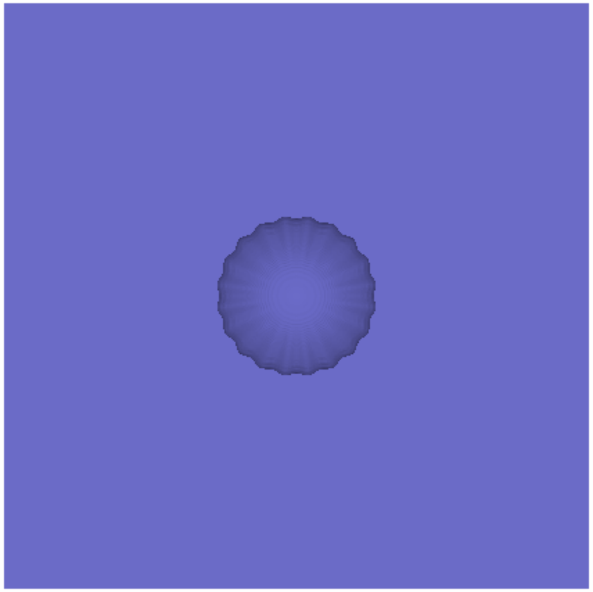 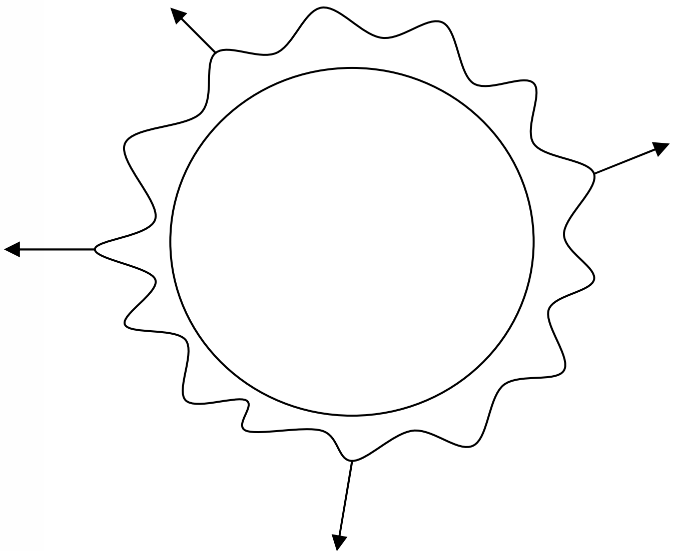

Why are perturbations amplified ?

# DROPLET IMPACT

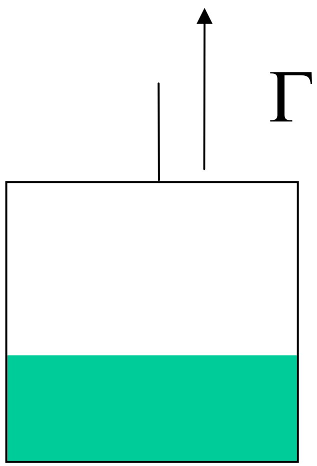


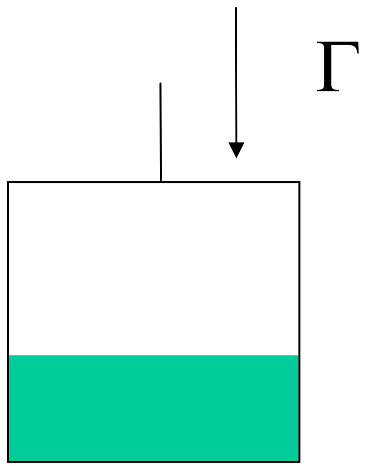


Standing in elevator
accelerated up
Feel « normal » gravity down
Stable

Standing in elevator
Accelerated down
Feel atttracted to roof
Effective gravity up: Unstable

Conclusion: Interface unstable when acceleration from light to heavy.

# DROPLET IMPACT

Select a numerically « nice » case:

Not too viscous (no splashing)
Not too large Re (too unstable)

A glycerine , 4 mm droplet falling at 2 m/s

$256^2$ Simulation ( 128 grid points/diameter )

Repeat at $128^2$ : same result

QuickTime™ et un
décompresseur Cinepak
sont requis pour visionner cette image.

Re = 450 ,

We = 533,

D/e = 4,

last frame

Ut/D = 1,81

# DROPLET IMPACT

QuickTime™ et un
décompresseur Cinepak
sont requis pour visionner cette image.

Low resolution

Re = 450 ,
We = 533,
D/e = 4,

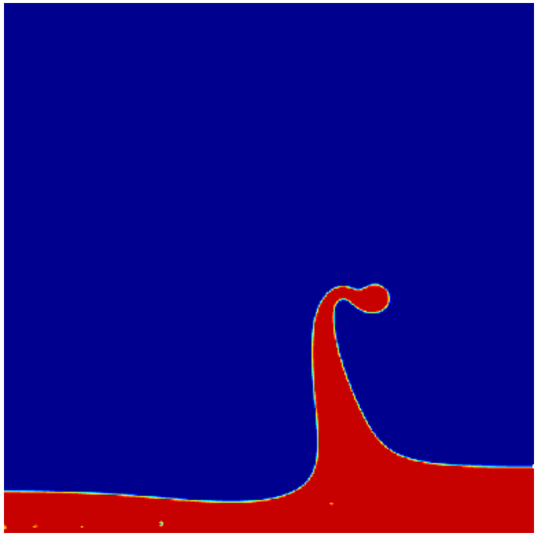

High resolution

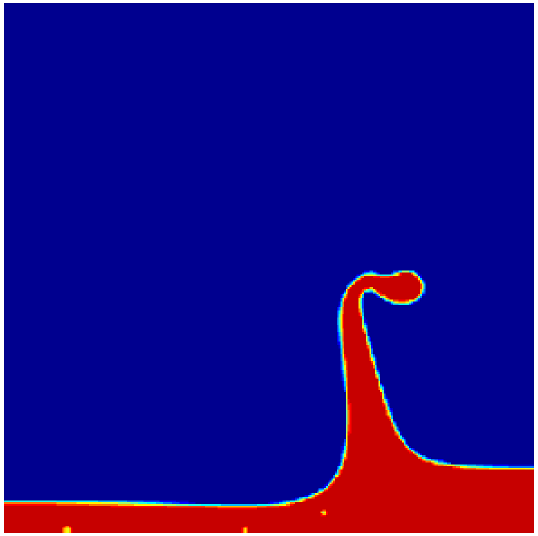

Low resolution

# DROPLET IMPACT

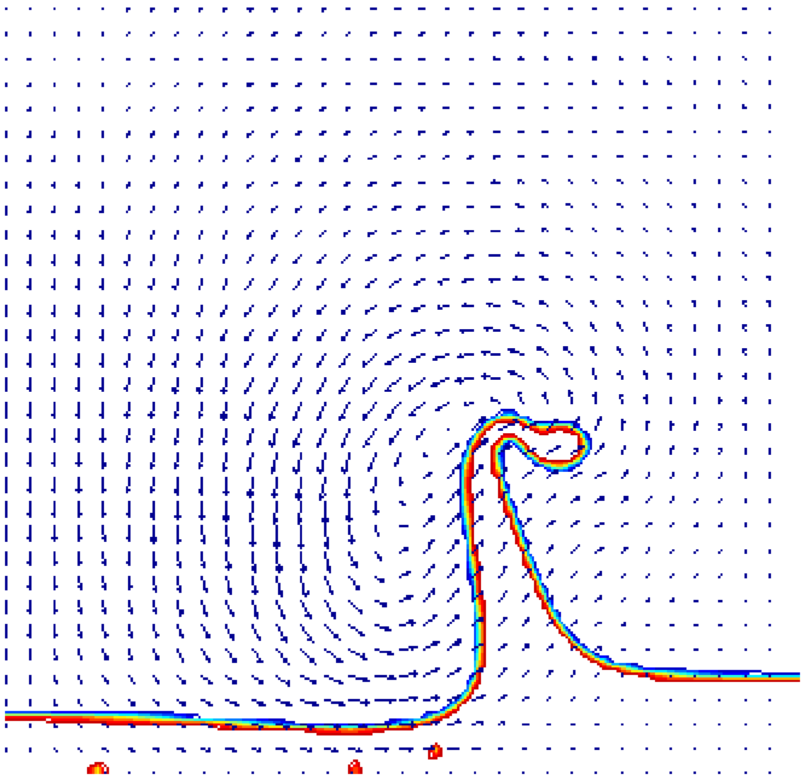

# DROPLET IMPACT

3D case, large resolution

$256^3$ Simulation ( 128 grid points/diameter )

Relatively small-amplitude initial azimuthal undulation

Notice reversal of curvature

Show 3D movie

# DROPLET IMPACT

Linear rate of growth in time (D. Gueyffier & SZ 1998, D. Gueyffier 2000)

# DROPLET IMPACT

Relatively larger-amplitude initial azimuthal undulation

Notice

-lift-up of fingers

-no adaptation of wavelength

Show 3D movie

# Thinner layer (D/h = 8) and larger horizontal extent (L_x/D = 4)

QuickTime™ et un
décompresseur Cinepak
sont requis pour visionner cette image.

# DROPLET IMPACT

The thinner layer creates a thinner corolla which now breaks !

Show 3D movie

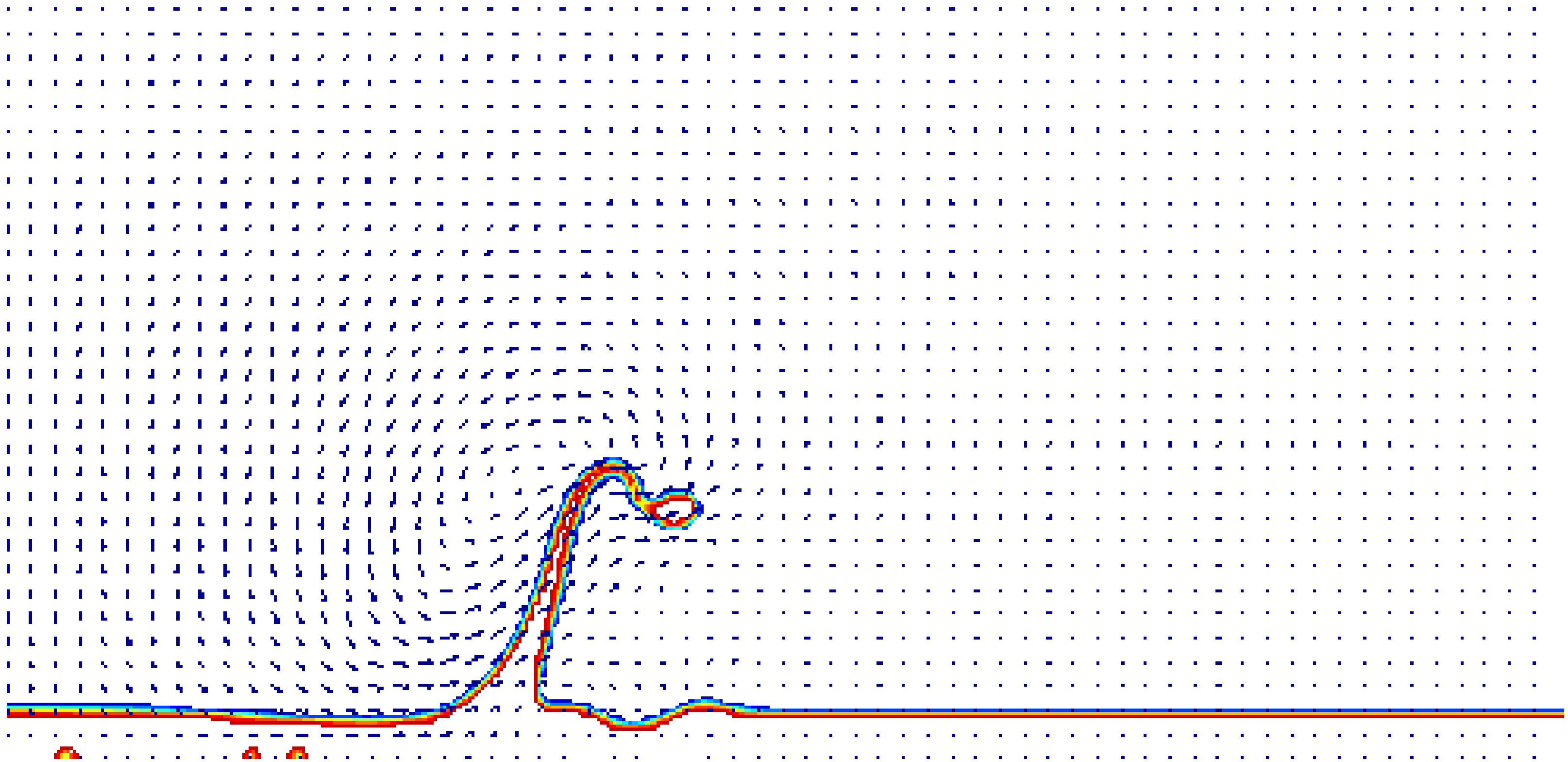

# DROPLET IMPACT

There is less uplift by the wind, so the corolla and the fingers are definitely drooping down.

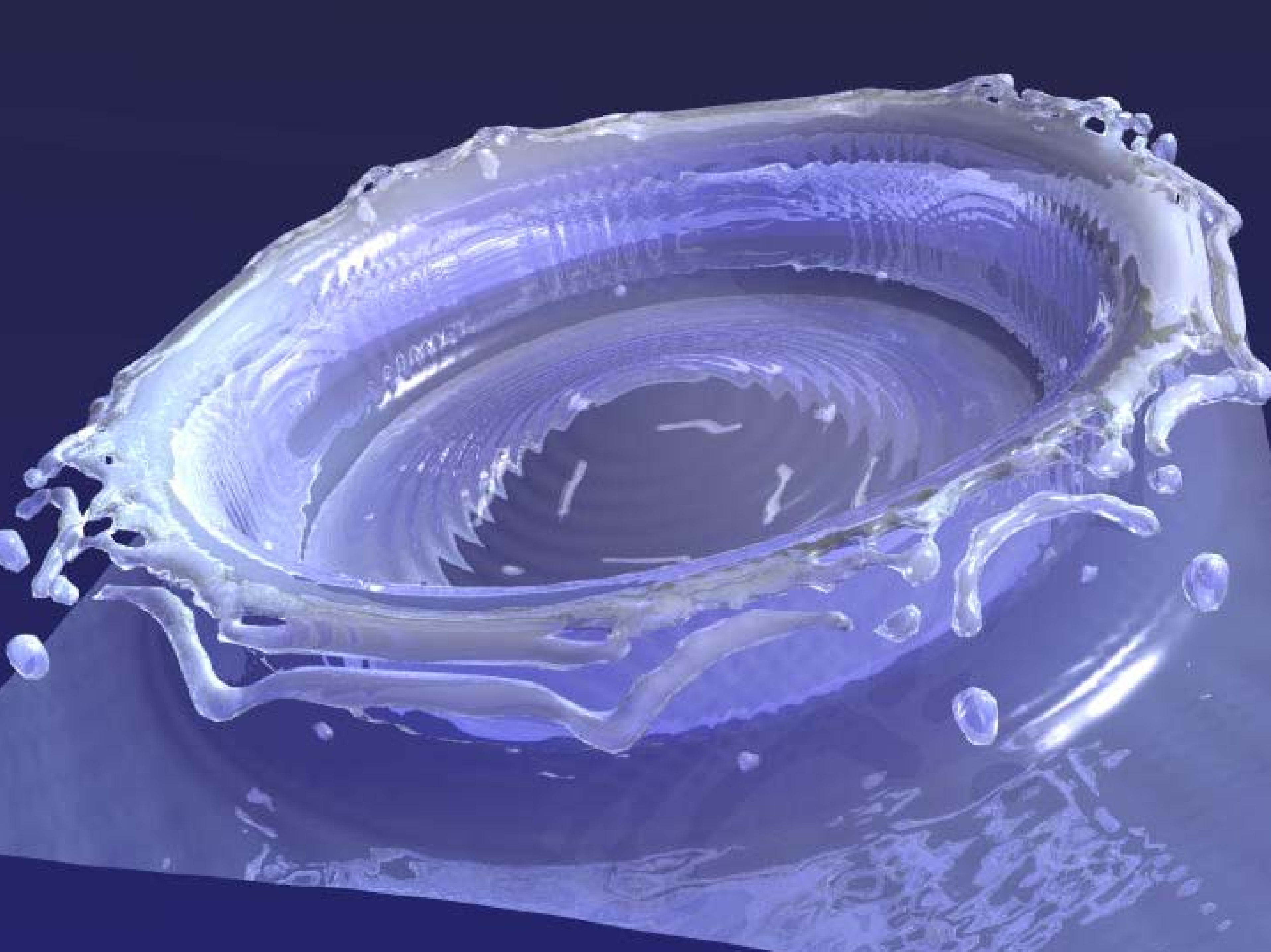

Conclusion: 2005 is not finished !

# CAVITATION BUBBLES

Bubbles tend to collapse asymetrically

- near walls
- in bubble clouds (see recent sonofusion controversy)

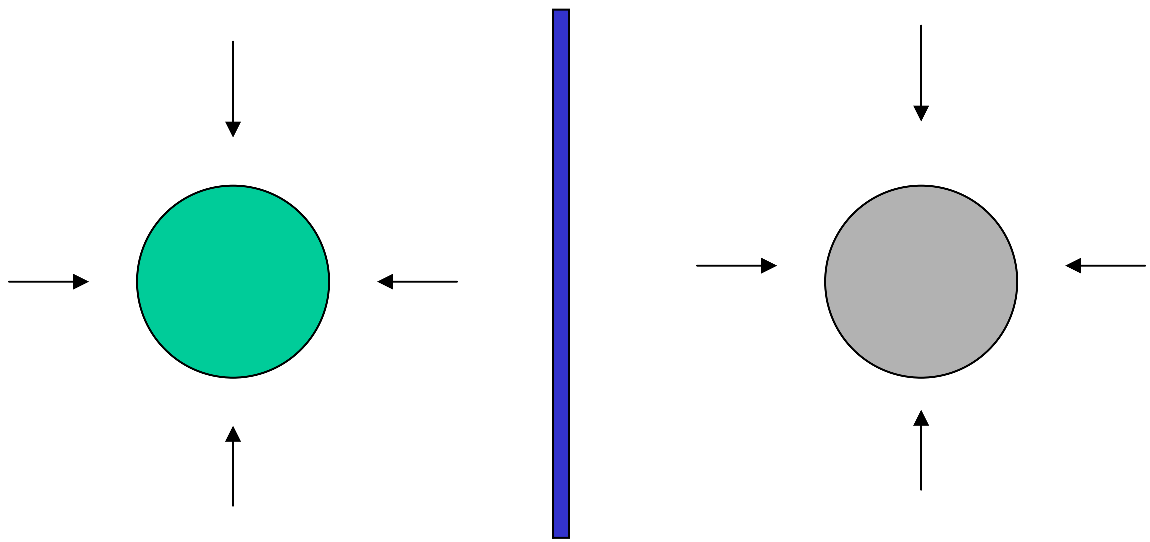

Collapsing bubble

Image bubble

Collapsing bubbles form jets.

Lauterborn ’s experiment:

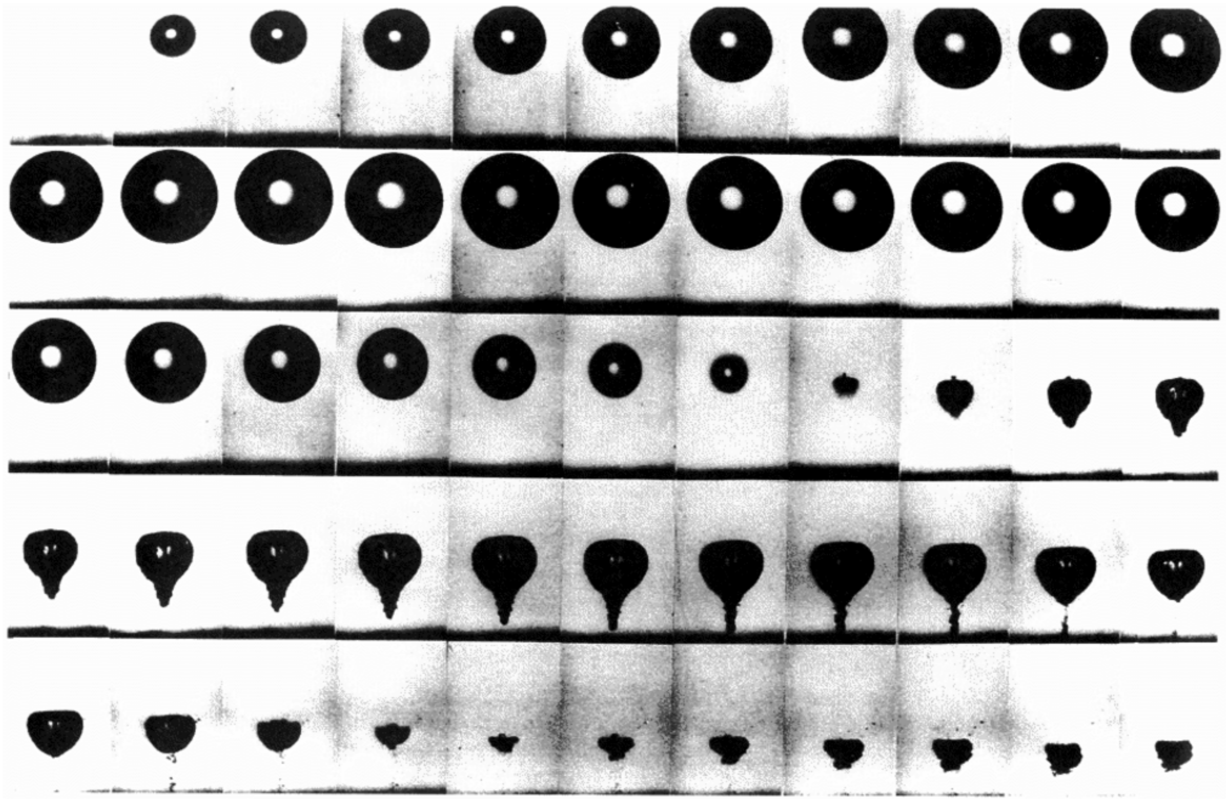

Use control points to extrapolate velocity field:

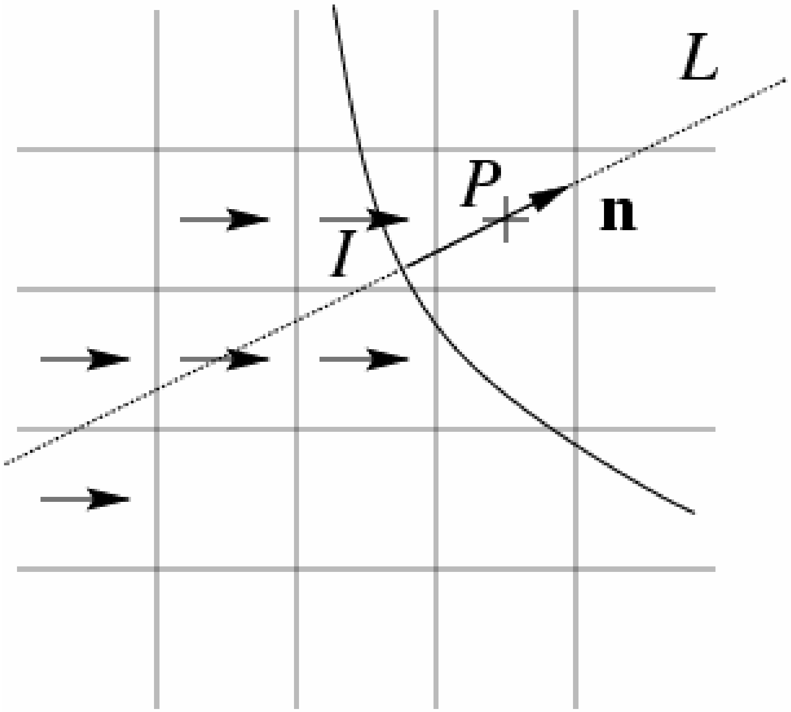

Free axisymmetric oscillations of a bubble:

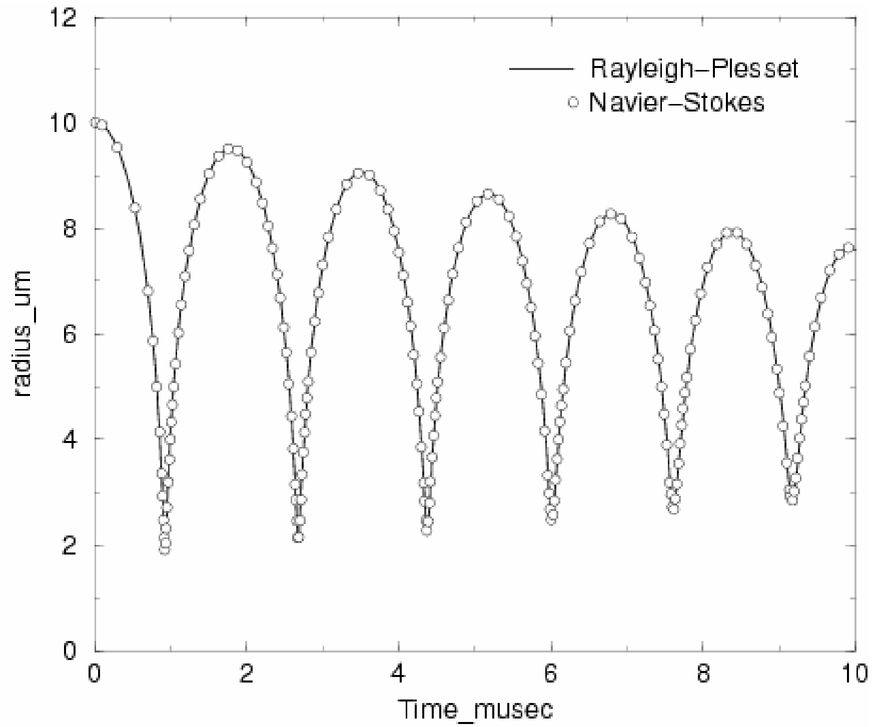

Comparison experiment/simulation

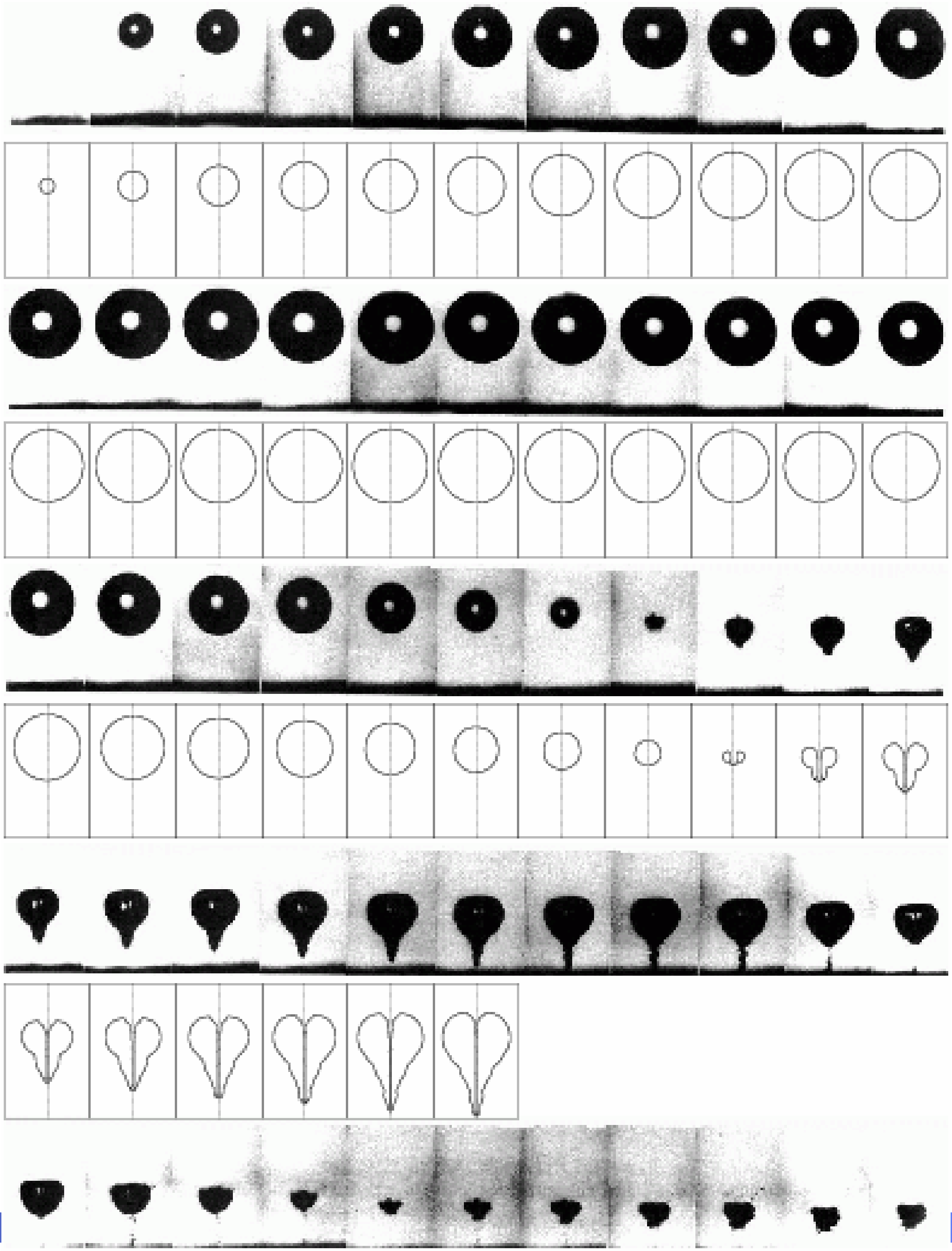

There is less energy in the real system after rebound:

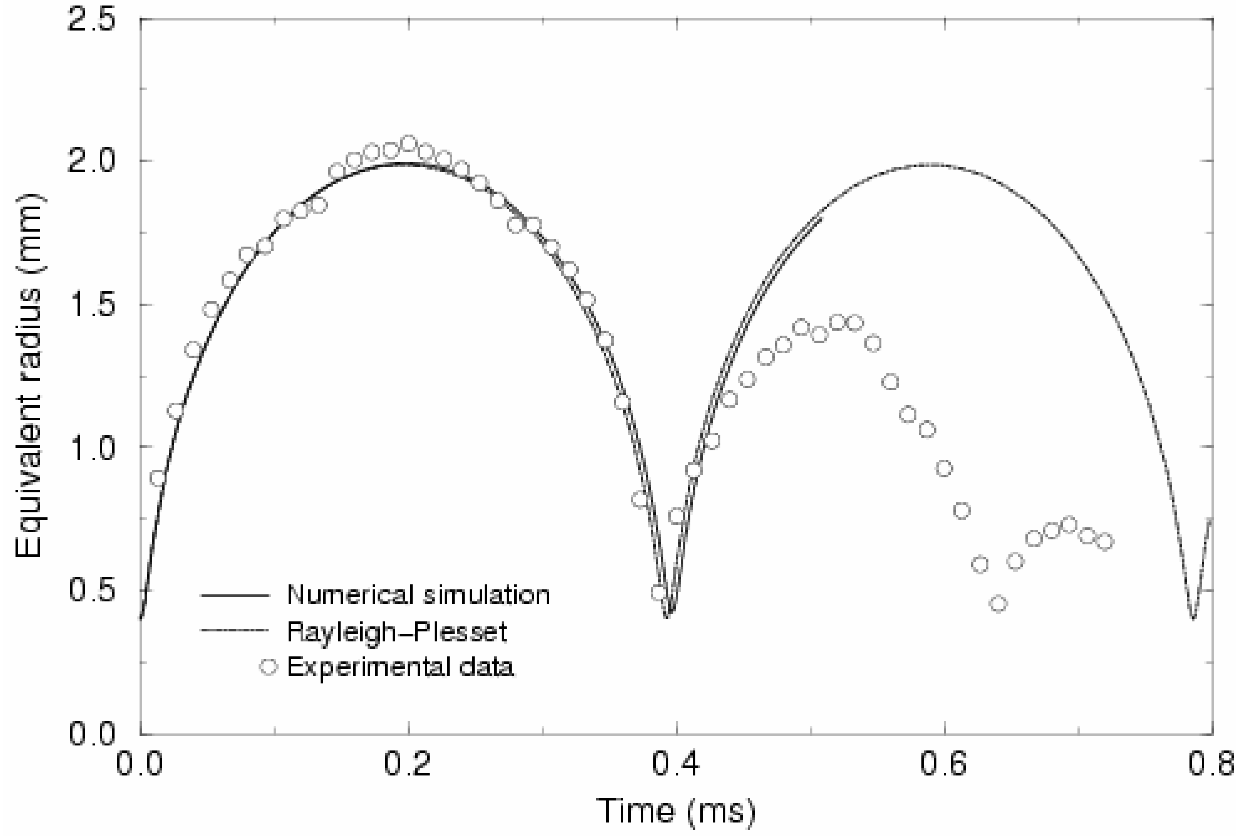

# Breaking bubbles

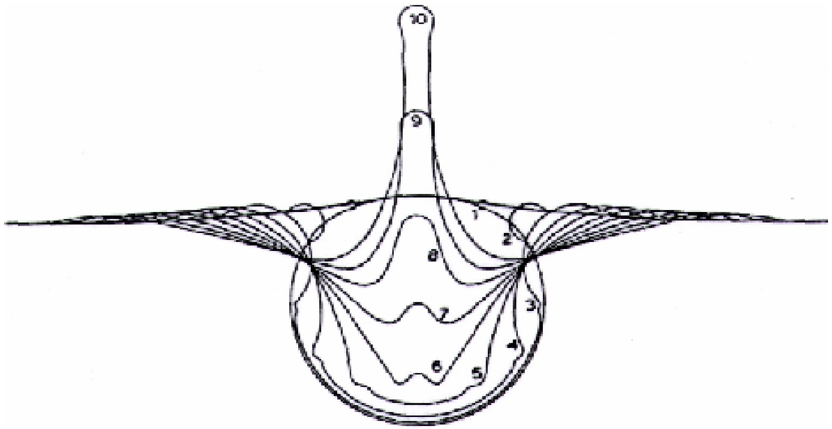


McIntyre

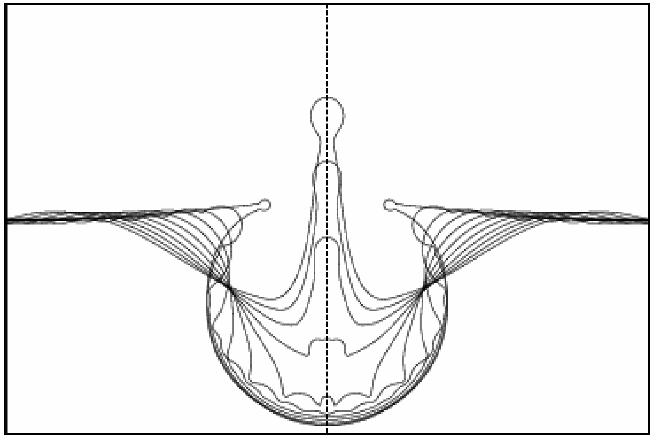

Simulation
(L. Duchemin)

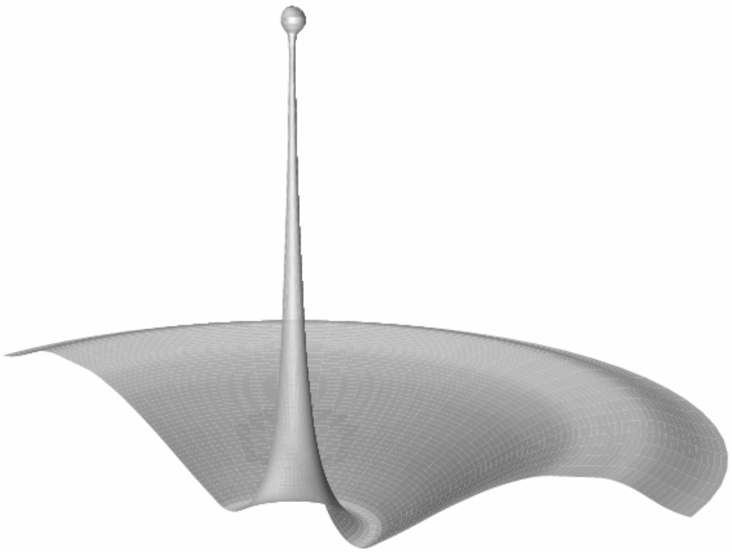

-- The marker method allows very accurate solutions of the free surface problem with viscosity.

- A critical ratio of distance to compression exists for jet formation near a wall. Surface tension effects remain to be added.

- Simulations of Bubble breaking phenomena show good agreement with experiment. A regime of high-speed, thin jets is found.

# LATTICE BOLTZMANN METHOD

Lattice Boltzmann Method (LBM)
Populations are averages, real numbers between 0 and 1.

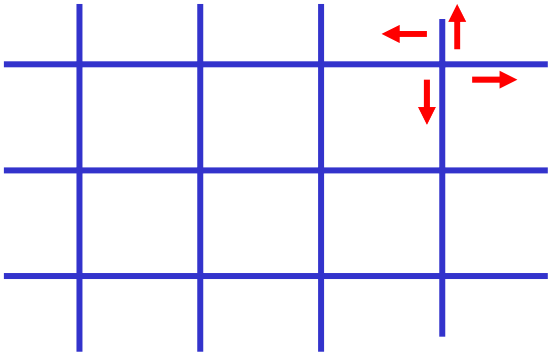

$$N_1(x+c_i, t+1) - N_1(x,t) = N_2(x,t)N_4(x,t) - N_1(x,t)N_3(x,t)$$

With three other equations for $N_{2,3 \text{ and } 4}$

# LATTICE BOLTZMANN METHOD

In general, the lattice Boltzmann populations obey the equation:

$$N_i(\mathbf{x}+c_i, t+1) - N_i(\mathbf{x}, t) = \Omega_i(\mathbf{N}(\mathbf{x}, t))$$

Where $\Omega_i = \Omega_i(\mathbf{N}(\mathbf{x}, t))$ is a complex collision operator.

Equations remain complex. A simpler method is obtained when
The right-hand side (the collision operator) is linearized

# LATTICE BOLTZMANN METHOD

Advantages of the LBM

- Simple formulation
- Easy parallelisation
- Automatic phase separation
- Automatic reconnection
- Exact mass and momentum conservation

# LATTICE BOLTZMANN METHOD

Applications of the LBM:

- Multiphase flow in porous media (Rothman, Adler).
- Bubbly flow (e.g work of Sundaresan, collaboration with Tryggvason).
- A commercial code (Powerflow of EXA corporation) exists using an extension of the LBM, mostly marketed to the automotive industry.

LATTICE BOLTZMANN METHOD

How to separate phases in a particle method?

•Introduce repulsive forces between A and B particles, or attractive forces between A and A particles.

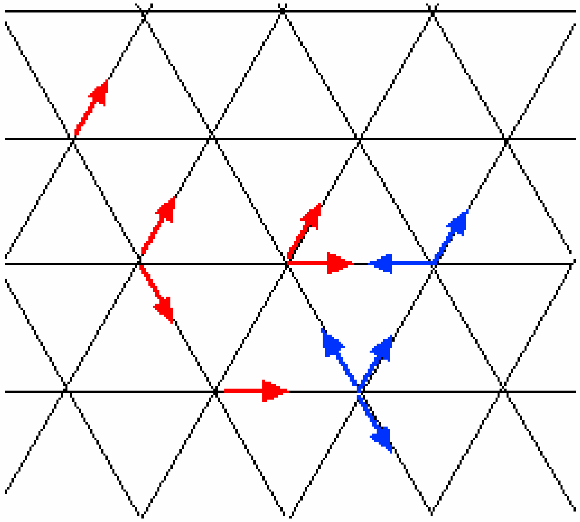

Models by

Rothman and Keller 1988
Chen et al. 1989

## LATTICE BOLTZMANN METHOD

Equations satisfied by the lattice Boltzmann method found by Chapman-Enskog expansion:

Mass conservation leads to :

$$\partial_t \rho + \nabla \cdot (\rho \mathbf{u}) = 0$$

(The LBM is compressible !)

Momentum conservation leads to :

$$\partial_t(\rho\mathbf{u}) + \nabla\cdot(\rho\mathbf{u}\otimes\mathbf{u}) = -\nabla p + \nabla\cdot\mathbf{S} + \sigma\kappa\delta_S\mathbf{n} + \left(\nabla\sigma\right)\delta_S + \rho\mathbf{g},$$

Where $$S_{ij} = \frac{\mu}{\rho}\left(\frac{\partial\rho u_j}{\partial x_i} + \frac{\partial\rho u_i}{\partial x_j} + \ldots\right)$$

Compare to the exact (compressible) equation:

$$S_{ij} = \mu\left(\frac{\partial u_j}{\partial x_i} + \frac{\partial u_i}{\partial x_j}\right) + \mu_2\left(\nabla\cdot\mathbf{u}\right)\delta_{ij}$$

# LATTICE BOLTZMANN METHOD

The jump conditions are not satisfied: true jump conditions (2D, constant σ)

a) velocity $[\mathbf{u}] = 0$

b) Momentum flux: $\left[\left(p\mathbf{1} + 2\mu\mathbf{D}\right)\cdot\mathbf{n}\right] = \sigma\mathbf{n}$

LBM jump conditions

a) Normal velocity $[\mathbf{u}\cdot\mathbf{n}] = 0$

b) Tangential velocity $[\rho\mathbf{u}\cdot\mathbf{t}] = 0$

c) Momentum flux: $\left[\left(p\mathbf{1} + \mathbf{S}\right)\cdot\mathbf{n}\right] = \sigma\mathbf{n}$

# LATTICE BOLTZMANN METHOD

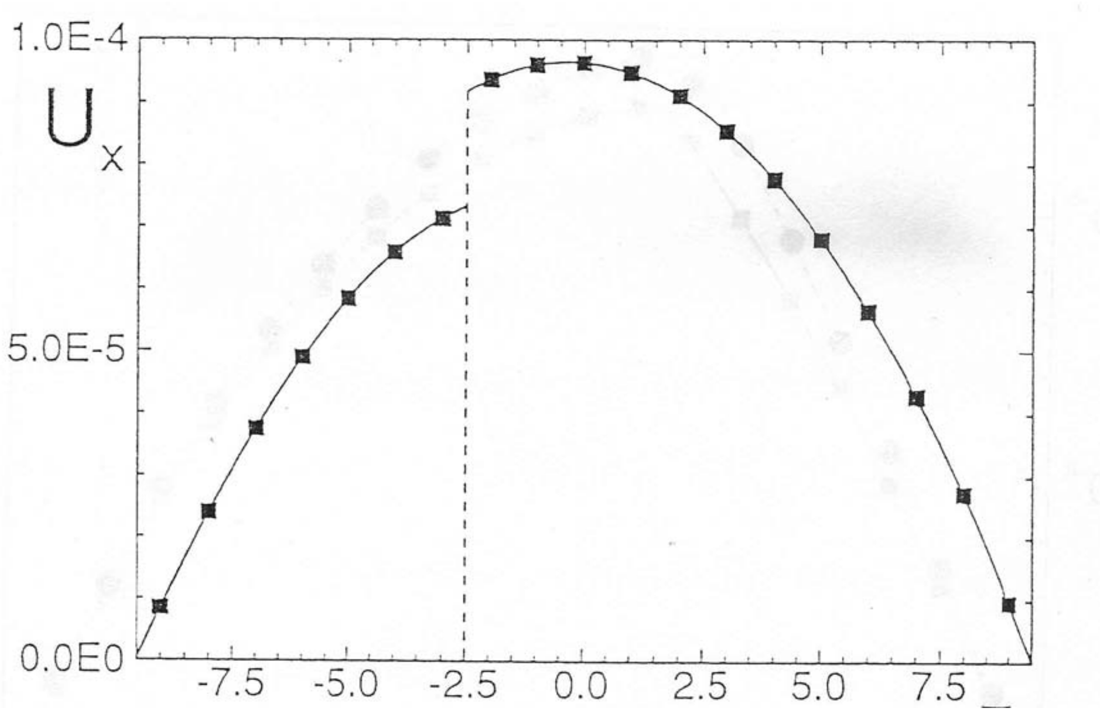


Double Poiseuille flow (Irina Ginzburg and Pierre Adler, unpublished) shows that $\rho u$ is continuous, not u.

## LATTICE BOLTZMANN METHOD

As a result the LBM is valid/useful only in special cases

-Re = 0
-Equal density
-Free surface

Examples: bubbles, flow in porous media.

QuickTime™ et un
décompresseur Vidéo 1 Microsoft
sont requis pour visionner cette image.

# Simulation, Youngseuk Keehm

QuickTime™ et un
décompresseur Vidéo 1 Microsoft
sont requis pour visionner cette image.

THE END !

# LATTICE BOLTZMANN METHOD

## LATTICE GAS CELLULAR AUTOMATA:HISTORY

- Kinetic theory models
- Statistical Physics Models
- Cellular Automata
- Hexagonal FHP gas
- Lattice Boltzmann Method
- Fixed point arithmetic Lattice Boltzmann Methods

LATTICE BOLTZMANN METHOD

Simplest lattice-gas cellular automaton model: the HPP

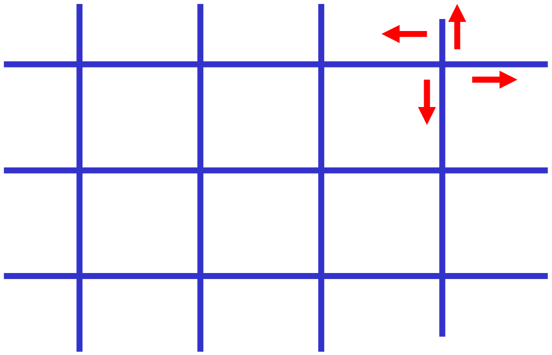

4 particles per node
One in each directions.

Particles collide and jump from cell to cell.
Momentum and particle number are conserved.

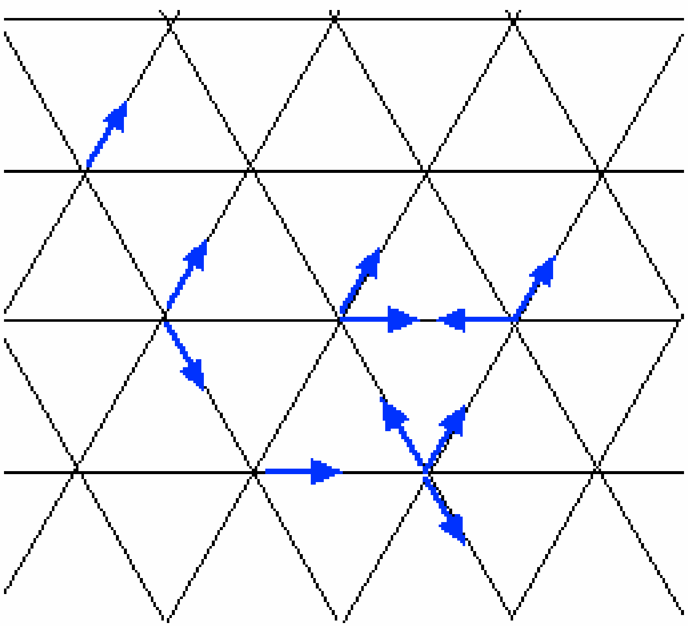

Hexagonal Frisch-Hasslacher-Pomeau (FHP) model:

6 particle velocities, 1 or 0 particle in each state.

Collision rules ensure conservation of mass and momentum and lead to large
scale equations ressembling Navier-Stokes.

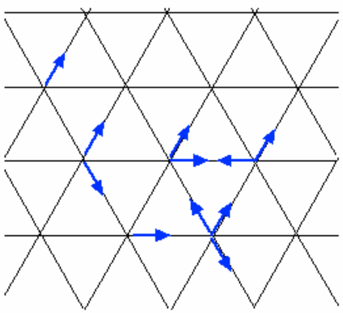

Model later extended to :

- •3 Dimensions
- •Two phase flow (two liquids and liquid-gas)
- •Models with thermal effects.
- •Thermal convection
- •Viscoelastic effects.

Difficulties:

- Considerable noise affects the results. Vorticity is most noisy, and interface positions fluctuate enormously
- The lack of Galilean invariance is difficult to fix. A fundamental problem of all « Cellular automata » type approaches to modelling is the absence of Noether-like theorems (equivalence between conservation laws and invariance under transforms).
- Other problems: compressibility effects, boundary conditions.

# FLOW IN POROUS MEDIA

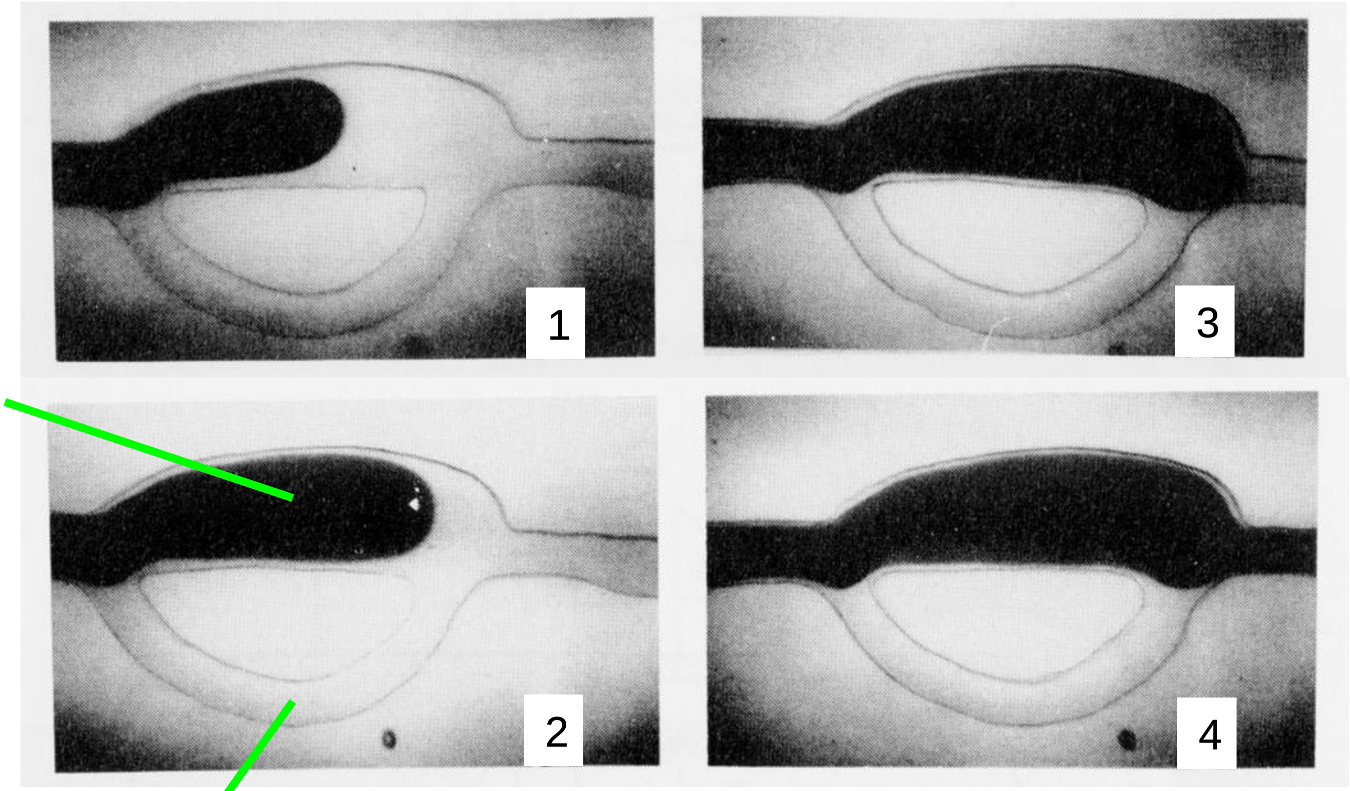


lab experiment by Chatzis and Dullien (1985).

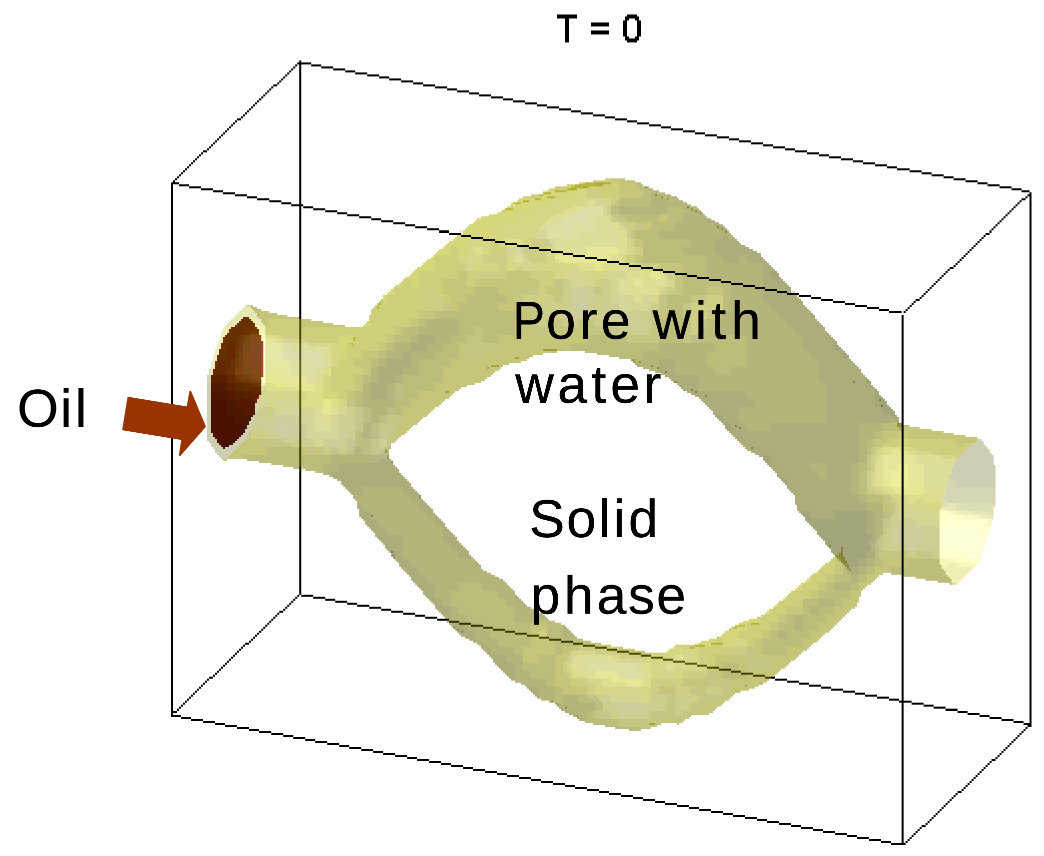


Simulation by Youngseuk Keehm , SRB

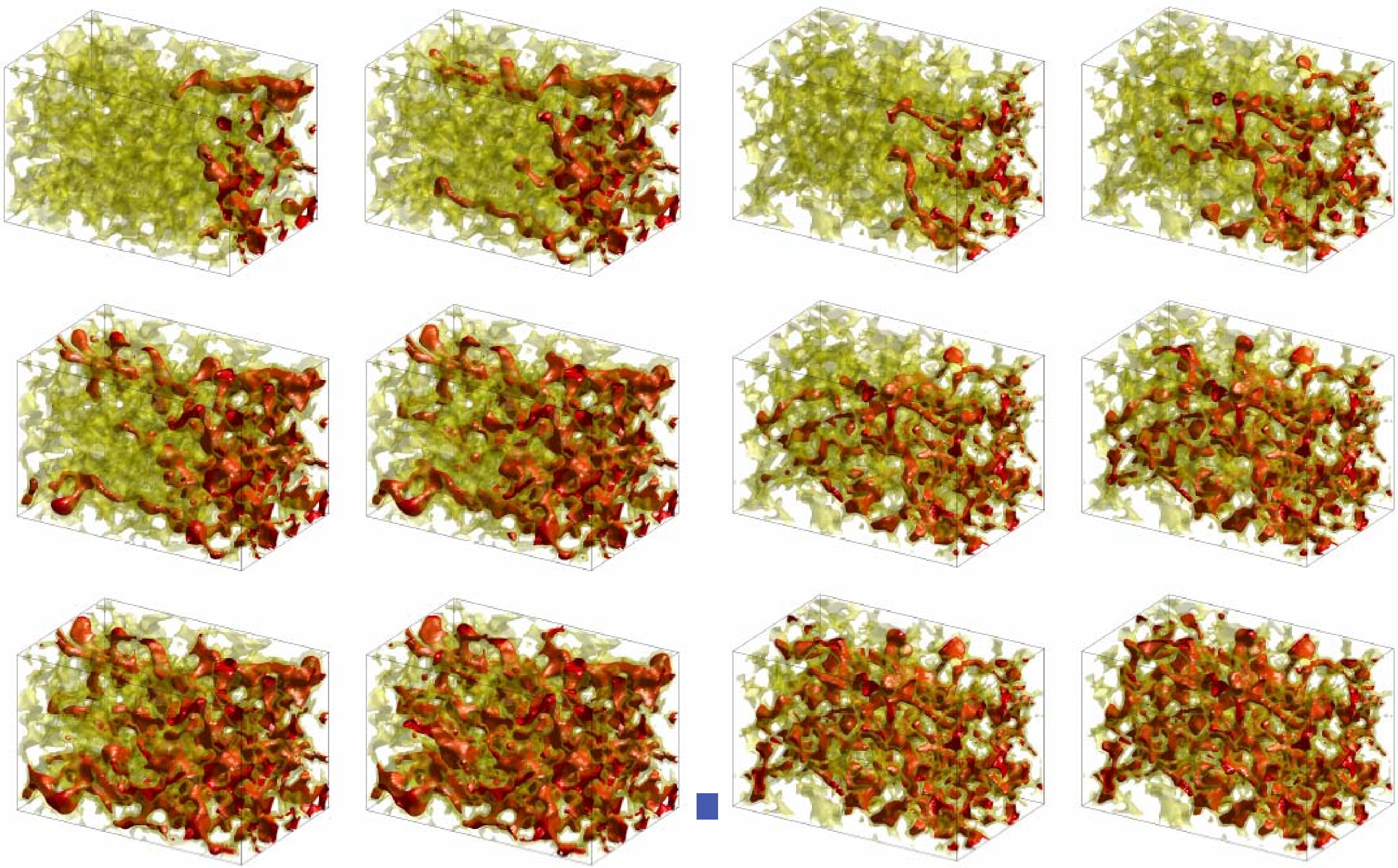

Low Pressure Gradient High Pressure Gradient

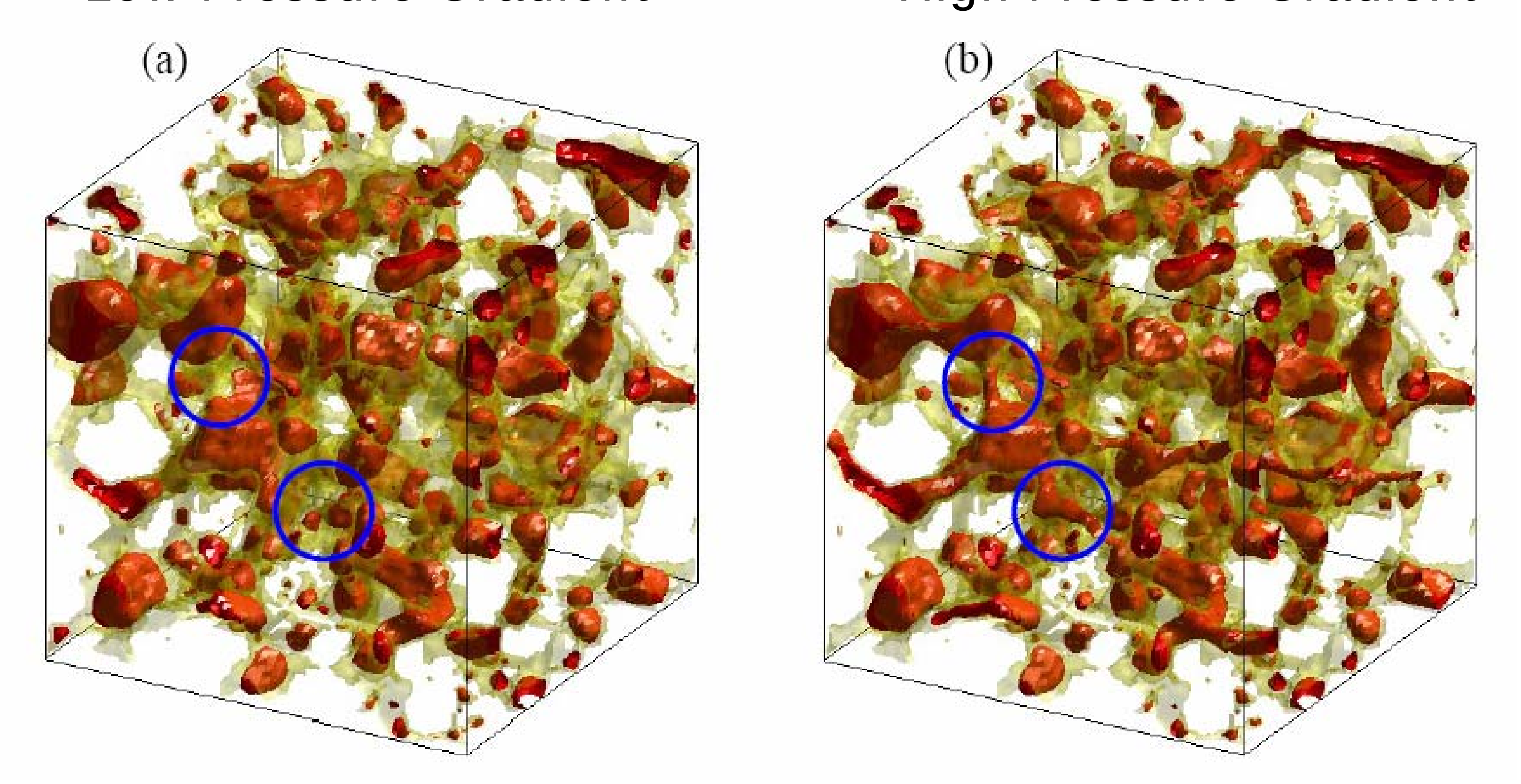

Low Pressure Gradient High Pressure Gradient